Atmospheric Degradation of Amines (ADA)

Summary Report:

Gas phase photo-oxidation of

2-aminoethanol (MEA)

CLIMIT project no. 193438

Claus Jørgen Nielsen, Barbara D'Anna, Christian Dye, Christian George, Martin Graus, Armin Hansel, Matthias Karl, Stephanie King, Mihayo Musabila, Markus Müller, Norbert Schmidbauer, Yngve Stenstrøm, Armin Wisthaler

Norsk institutt for luftforskning
Norwegian Institute for Air Research
NILU

Atmospheric Degradation of Amines (ADA)

Summary Report:

Gas phase photo-oxidation of 2-aminoethanol (MEA)

Claus Jørgen Nielsen, Barbara D'Anna, Christian Dye, Christian George,
Martin Graus, Armin Hansel, Matthias Karl, Stephanie King,
Mihayo Musabila, Marcus Müller, Norbert Schmidbauer,
Yngve Stenstrøm, Armin Wisthaler

The European Photochemical Reactor, EUPHORE , in Valencia, Spain

Preface

Development and testing of amine-based technology for CO_2 capture is on-going in Norway. The technology may have effects on the environment through amine emissions to the atmosphere. A screening study[1] has revealed that the photo-oxidation of amines emitted to air may result in malevolent compounds with unwanted effects on the environment and human health. The effects are difficult to evaluate because little is known about these compounds and their production rates in the amine photo-oxidation. The *Atmospheric Degradation of Amines* project – ADA – has undertaken a systematic experimental study of the atmospheric photo-oxidation of 2-aminoethanol (MEA),[2] $H_2NCH_2CH_2OH$ (CAS: 141-43-5) and addresses open issues from the project "Amines, emissions to air - A screening project for environmental effects".

The overall objective was to contribute to the understanding of the atmospheric degradation of amines emitted to the atmosphere. The specific targets were:

- To identify the gas phase photo-oxidation products of MEA under various natural atmospheric conditions.
- To quantify branching ratios and the most important long-lived products in the gas phase photo-oxidation of MEA.
- To verify/update the existing atmospheric photo-oxidation schemes for MEA and to account for all products resulting from the OH initiated oxidation under natural conditions.
- To assess the conditions for aerosol formation during the gas phase photo-oxidation of MEA, and to characterize and quantify the aerosol formation.
- To establish an experiment/analysis protocol for future screening studies of amines.

The present report summarises the findings and conclusions from the ADA study on the atmospheric photo-oxidation of MEA. The project has achieved its targets related to MEA as defined in "Amines, emissions to air - A screening project for environmental effects".

The ADA project was financed by CLIMIT, MASDAR and Statoil ASA. The project progress was actively monitored by a Steering Committee comprising the industry partners and the project manager, Prof. Claus Jørgen Nielsen (CTCC, UiO), who headed the Steering Committee and who also held the Steering Committee voting power. CLIMIT exercised observatory status at the Steering Committee meetings.

---

[1] Amines, emissions to air - A screening project for environmental effects, http://co2.nilu.no/ProjectReports/tabid/2549/language/en-US/Default.aspx

[2] The list of trivial- and trade names are plenty: β-Aminoethanol; β-Aminoethyl alcohol;

[2] The list of trivial- and trade names are plenty: β-Aminoethanol; β-Aminoethyl alcohol; β-Ethanolamine; β-Hydroxyethylamine; 1-Amino-2-hydroxyethane; 2-amino-1-ethanol; 2-Aminoethanol; 2-Aminoethyl alcohol; 2-Ethanolamine; 2-Hydroxyethanamine; 2-Hydroxyethylamine; Aminoethanol; Colamine; ETA; Envision Conditioner PDD 9020; Ethanolamine; Ethylolamine; Glycinol; MEA; MEA (alcohol); MEA-LCI; Mealan; Monoethanolamine; Olamine; Seramine.

2

Contents

4

Executive Summary

The atmospheric gas phase photo-oxidation of 2-aminoethanol ($NH_2CH_2CH_2OH$, MEA) has been studied under pseudo natural conditions at the European Photochemical Reactor, EUPHORE, in Valencia, Spain. The experiments were carried out under different, relevant NOx conditions and initial MEA gas phase mixing ratios of 0.1 to 1 ppmV. The photo-oxidation was monitored *in situ* by FT-IR and on-line by PTR-TOF-MS, and samples were collected on various adsorbents for subsequent off-line analysis. The formation of particles was monitored by SMPS and AMS on-line instruments and filter sampling followed by analysis with LC/HRMS(TOF).

Atmospheric photo-oxidation is dominated by the OH radical which reacts with MEA by abstracting a hydrogen atom. All major photo-oxidation products have been identified and quantified, and limits to the branching ratios in the initial H-abstraction reaction obtained. Based on the results from on-line and in situ instrumentation it is found that more than 80 % of the reaction between MEA and OH radicals takes place at $-CH_2-$, while less than 10 % occurs at $-NH_2$, and less than 10 % at $-CH_2OH$. The major products (>80 %) in the photo-oxidation are formamide (NH_2CHO) and formaldehyde (CH_2O), of which the latter has a short atmospheric lifetime. Minor products (<10 %) are the short-lived amino acetaldehyde (NH_2CH_2CHO) and the longer lived 2-oxo acetamide ($NH_2C(O)CHO$).

The nitrosamine, $ONNHCH_2CH_2OH$ (2-(*N*-nitrosoamino)-ethanol) and the nitramine, $O_2NNHCH_2CH_2OH$ (2-(*N*-nitroamino) ethanol) may both be carcinogenic photo-oxidation products of MEA emitted to the atmosphere. Nitrosamines were not detected in any of the experiments. The nitramine, $O_2NNHCH_2CH_2OH$, was confirmed as product in the experiments. The yield depends upon the mixing ratio of NOx. For rural regions with NOx levels of 0.2-10 ppbV, less that 3 ‰ of emitted MEA will end up as the nitramine.

The photo-oxidation of MEA was found to give rise to ozone and significant formation of particles. Aerosols were formed immediately after the exposure of the chamber to sunlight; simulations of the chamber experiments show that, depending on the initial conditions, between 20 and 50 % of MEA removal from the gas-phase is due to reaction with OH radicals, between 10 and 40 % is converted into particle mass (gas-to-particle conversion) during the photo-oxidation experiments, while the remaining 30 to 70 % of the initial MEA amount is lost to the walls or by dilution through replenishment flow.

Exposure to fine particulate matter with diameter below 2.5 µm (PM2.5) is widely recognized as health concern and new European legislation has been enforced to reduce levels of fine particles. In the atmospheric boundary layer wetted surfaces (buildings, particles, and cloud droplets) are present which will provide a medium for the uptake of MEA. Atmospheric dispersion model calculations including the gas phase/liquid phase partitioning of MEA and particle formation processes are necessary to estimate the exposure of the population and the environment to particles and oxidation products forming from MEA.

6

Atmospheric Degradationof Amines (ADA)

Summary Report: Gas phase photo-oxidation of 2-aminoethanol (MEA)

1   Theoretical photo-oxidation schemes

Detailed theoretical schemes for the atmospheric photo-oxidation of MEA ($H_2NCH_2CH_2OH$, 2-aminoethanol) have previously been reported.[1] The schemes are based on generic atmospheric photo-oxidation pathways for hydrocarbons[2-3] and experimental data for amines from the literature.[4-19]

The atmospheric photo-oxidation of MEA is dominated by reaction with OH radicals although Cl atoms may constitute a minor sink in costal regions and NO_3 radicals may contribute during night-time. There are 4 possible sites at which the initial reaction – a hydrogen abstraction – can take place in MEA: two in the –CH_2OH group leading to the same products, one in the –CH_2– group, and one in the –NH_2 group.

Schemes 1.1-1.3 show the expected major reaction routes following the initial hydrogen abstraction. Intermediate compounds are highlighted in colour coded boldface types (**black**: expected atmospheric lifetime <1 day; **blue**: expected atmospheric lifetime >3 days at 60° N; **red**: expected to be toxic/carcinogenic).
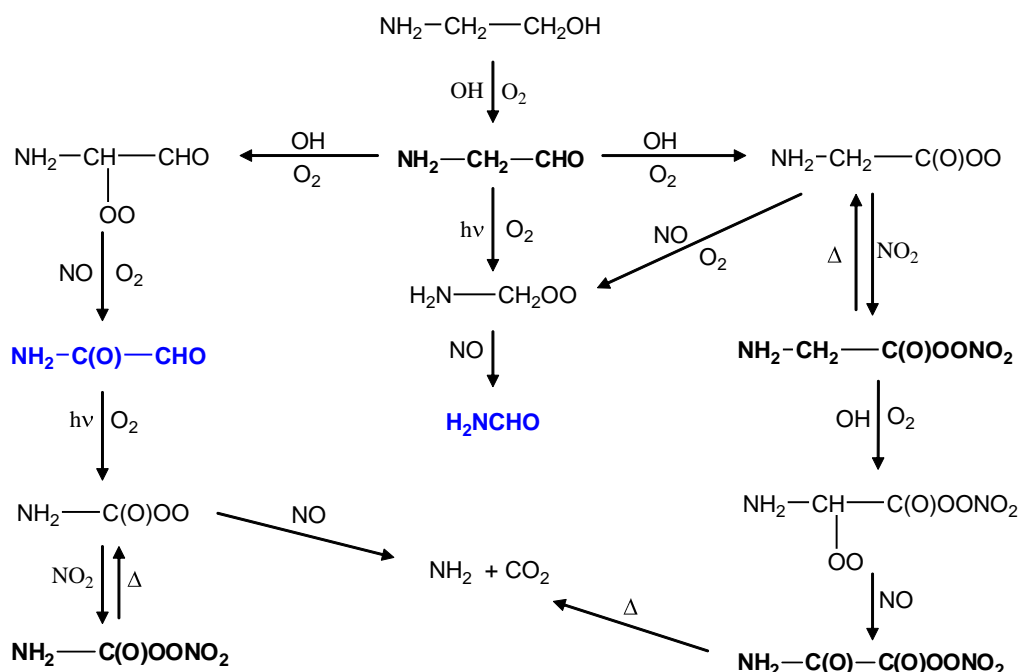
Scheme 1.1. Expected atmospheric degradation of MEA following hydrogen abstraction from the -CH_2OH group (adapted from Ref. 1).

The major products with expected atmospheric lifetimes >3 days at 60° N resulting from initial H-abstraction from the -CH_2OH group (Scheme 1.1) include

NH_2CHO (formamide, CAS: 75-12-7) and $NH_2C(O)CHO$ (2-oxo acetamide, CAS: 60939-21-1).

The major products with expected atmospheric lifetimes >3 days at 60° N resulting from initial H-abstraction from the $-CH_2-$ group (Scheme 1.2) include NH_2CHO (formamide, CAS: 75-12-7) and $NH_2C(O)CH_2OH$ (2-hydroxy acetamide, CAS: 598-42-5). In addition, CH_2O (formaldehyde, CAS: 50-00-0) will be formed in amounts equal to that of formamide.
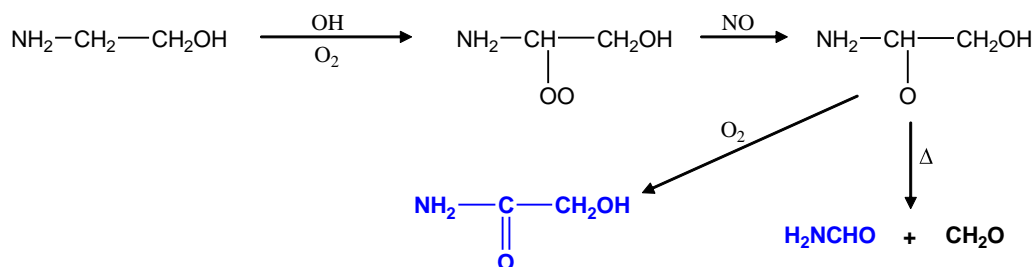
Scheme 1.2. Expected atmospheric degradation of MEA following hydrogen abstraction from the $-CH_2$-group (adapted from Ref. 1).

The major products expected to result from initial H-abstraction from the $-NH_2$ group (Scheme 1.3) include $ONNHCH_2CH_2OH$ (2-(N-nitrosoamino)-ethanol, CAS: 98033-27-3), which will undergo rapid photolysis during <u>daytime</u>, $O_2NNHCH_2CH_2OH$ (2-(N-nitroamino)-ethanol, CAS: 74386-82-6), and $HN=CHCH_2OH$ (2-imino ethanol, CAS: 724427-16-1(Z), 724427-18-3(E)). Essentially experimental data are available on the atmospheric fate of imines in general and of $HN=CHCH_2OH$ in particular.
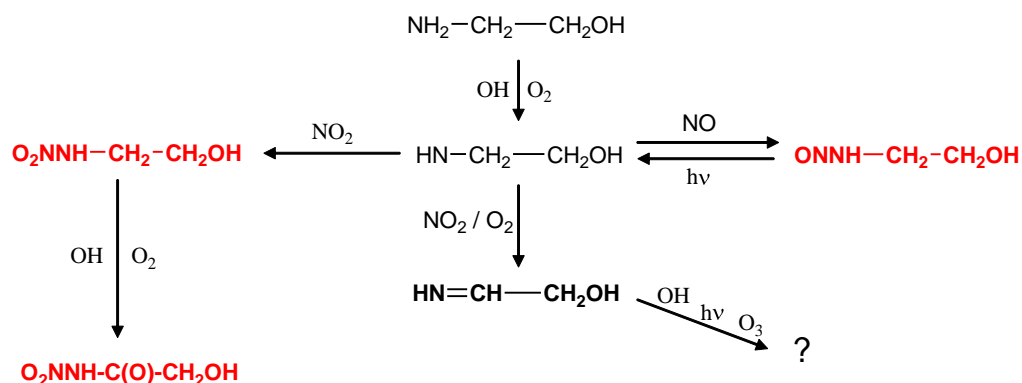
Scheme 1.3. Expected atmospheric degradation of MEA following hydrogen abstraction from the NH_2-group (adapted from Ref. 1).

2 Experimental activities

The ADA project included several activities: photo-oxidation studies at EUPHORE, development of an aerosol model, organic synthesis of MEA isotopomers and reference compounds such as *N*-nitro amines, registration of absolute infrared absorption cross sections, and development of analytical methods.

2.1 Off-line analytical methods

All off-line techniques used in this project collect both gas phase and particulate matter (aerosols). For this reason the off-line analysis results are not directly comparable with any of the on-line measurement results. A general picture should be that the off-line measurements are systematically higher in concentrations than the data obtained by on-line techniques.

An important property by the off-line techniques is the inherent higher number of analytical identification points compared to the on-line techniques. This enables the definitive confirmation of the chemical compounds identified by the on-line techniques. The analytical methodologies are briefly outlined in the following.

Amines. The amine analyses were performed with an in-house method which is based on derivatisation to improve the behaviour towards reversed phase chromatography. Small punches of the filter samples were prepared by adding a buffer solution and the derivatizing agent in a vial. After at least 4 hours reaction time, a sample aliquot was subjected for chemical analysis. The analyses were performed by liquid chromatography (HPLC) combined with high resolution mass spectrometry, and isotope labelled internal standards were used for quantification.

The amine method has, during the project, been upgraded by adaption to the high concentrations of amines present in the chamber. The validation of the upgraded method was done by preparing small punches from the exposed filter. Derivatisation recovery of spiked monoethanolamine is normally higher than 97% and the relative standard deviation obtained by analyzing 7 punches from chamber experiments the 10th of May, was 13%. The corresponding relative standard deviation for ethylamine on the 8th of September was 17% (n=3). The amine collection efficiency is normally better than 95% on the first filter in the filter package.

Carbonyl compounds. The sampling is performed by drawing air through a cartridge which contains 2,4-dinitrophenylhydrazine (2,4-DNPH)-coated silica packed in a polyethylene tube. Aldehydes and ketones react with the acified 2,4-DNPH to form the corresponding hydrazones. After exposure the cartridge is eluted with acetonitrile, and the sample extract is analysed by reversed phase liquid chromatography (HPLC) combined with serial connected diode array detector (UV) and high resolution mass spectrometry (HRMS).

Nitrosamines. The nitrosamines were analysed by an in-house validated method based on applications found in the literature. The samples were collected on

Thermosorb/N adsorbent tubes. The analyses were performed by liquid chromatography (HPLC) combined with high resolution mass spectrometry using $^{13}C_2$–labeled N-nitrosodimethylamine and D_{10}-labeled N-nitrosodiethylamine as internal standards.

Nitramines. The nitramines were analysed by the same principles as the carbonyl compounds. The acetonitrile extracts needed extra workup steps before the chemical analysis. The typical precision obtained by analysis of spiked samples was 15% relative standard deviation (n=4) and a spike recovery of 25% for methylnitramine and 35% for ethylnitramine. The limit of detection is approximately 1 ppb with a good potential for improvement The nitramine data given are recovery corrected. Figure 2.1 shows part of an ion chromatogram obtained from a sample taken during a photo-oxidation reference experiment with ethylamine.
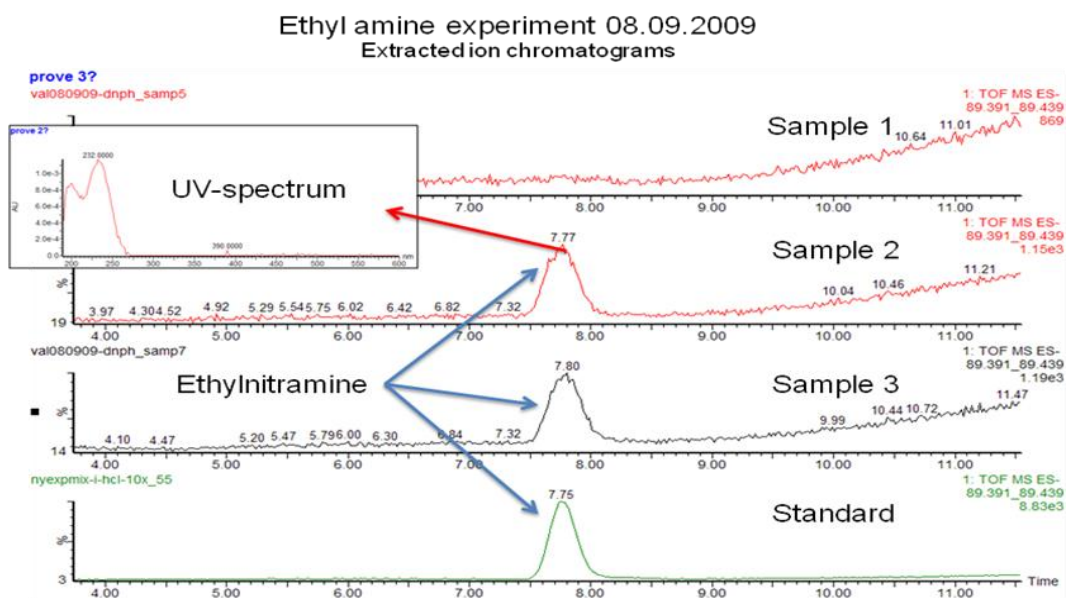
Figure 2.1. HPLC-HRMS extracted ion chromatogram from a photo-oxidation experiment with ethylamine. Data from September 8, 2009.

VOC. Tenax TA adsorption tubes sampled with an air flow of 0.2 liters per minute for 60 minutes are used as a broad-band non target method. Sampling on Tenax and analysis with thermo desorption followed by GC-MS-TOF covers volatile compounds with a boiling point from about 40 to 250 °C. The sample volume and the sample flow should be adapted to the target compounds. With a flow rate less than 100 ml/min and a total flow less than 5 liters even very volatile compounds like pentane can be trapped and analysed quantitatively. Since the main focus was not the very volatile solvents but molecules containing Nitrogen and/or Oxygen the flow rate and save-sampling volume were adapted to that.

2.2 On-line and *in situ* analytical instrumentation

PTR-TOF-MS. Proton Transfer Reaction - Mass Spectrometry (PTR-MS) is a highly sensitive, real-time analytical technique for detecting volatile organic compounds

(VOCs) in air. PTR-MS combines the concepts of soft, non-fragmenting chemical ionization and of highly sensitive and quantitative product ion formation in an ion drift tube. H_3O^+ primary ions are produced in a hollow cathode ion source and injected into a drift tube which is continuously flushed with sample air. In the drift tube, the H_3O^+ primary ions undergo proton transfer reactions with organic trace analytes following simple pseudo-first order reaction kinetics. In most cases, protonated analyte molecules are quantitatively formed and mass spectrometrically detected one mass unit higher than the neutral compound. The newly developed High-Resolution Proton-Transfer-Reaction Time-of-Flight Mass Spectrometer (PTR-TOF-MS) has a mass resolving power of m/Δm of ~ 5000 (FWHM) and a 5-to-10 ppm mass accuracy which allows to determine the exact mass and thus elemental composition of the analyte molecules. VOCs are quantitatively detected with a detection limit of ~ 10 pptV for a 1 minute signal integration time. An accuracy of 5 % is obtained using calibrated VOC mixtures; the uncalibrated accuracy is on the order of 25 %.

AMS. The time-of-flight Aerodyne Aerosol Mass Spectrometer (AMS) is an innovative instrument that allows real-time and *in situ* analysis of fine and ultrafine particles. The instrument investigates size distribution and chemical composition of particles between 0.03 to 1mm on a 1 min basis. The methodology used within c-TOF AMS is fully described in Drewnick *et al.*[20] The particles are sampled through a critical orifice (diameter 100μm) at 80 cm^3 min^{-1} and focused by an aerodynamic lens which blocks all particles larger than 1mm in diameter. Then they enter a vacuum chamber where a mechanical chopper allows a packet of particles (beam chopped) to be accelerated according to their vacuum aerodynamic diameter (D_{va}) and thereby giving size distribution data. The particles are then sent to the vaporization-ionization chamber where the non-refractory (NR) components of the particles are flash-vaporized on a hot surface (~600 °C) and ionized by electron impact (70 eV). Resultant positively charged ions are guided into the time-of-light mass spectrometer, allowing 0.5 unit mass resolution. The collected mass spectra (m/z from 4 to >350 in a minute scale) give information on the chemical composition (i.e., nitrate, sulphate, chloride, potassium, ammonium, aliphatic organic, PAHs) using the "fragmentation table". Using default parameters (70eV for the electron impact ionisation) fragmentation of the aliphatic organic fraction is important and precise identification of a parent compound cannot be performed. Such limitation can be minimized by post-analysis of the aliphatic organic mass fraction using PMF (positive Matrix factorisation analysis). This methodology has been successfully applied to separate hydrocarbon like material from traffic related emissions, and oxygenated and biomass burning particles.[21] Another possible alternative is to reduce the electron impact ionisation (ex. from 70 to 30eV), reducing therefore the fragmentation of the amines and their degradation products.

FT-IR. Chamber B is equipped with a Nicolet Magna 550 FTIR spectrometer coupled with White multi-reflection mirror system for in situ analysis adjusted to give an optical path length of 553.5 m. FTIR spectra were recorded every five

minutes by co-adding 280 interferograms with a resolution of 1.0 cm^{-1}. Happ-Genzel apodization was used in the Fourier transformation. The retrieval of trace gas volume mixing ratios were carried out semi-automatically employing the MALT program.[22] This method simulates the spectrum of the mixture of absorbing species from a set of initial concentrations and reference spectra and then varies the concentrations iteratively to minimize the residual between the measured and simulated spectrum. In the spectrum calculation, true absorption coefficients are used if available, otherwise high resolution spectra can be used as a good approximation. The spectral data needed in the fitting procedure were taken from the HITRAN 2008 database (H_2O, CO, NO, NO_2, CO_2, CH_4);[23] for MEA and formamide experimental IR spectra were used.

FT-IR spectra (4000-400 cm^{-1}) of MEA vapour in a 23.0 ± 0.1 cm gas cell with KBr windows were recorded at 298 ± 2 K using a Bruker IFS 66vs spectrometer employing a nominal resolution of 1.0 cm^{-1} and Boxcar apodization of 128 co-added interferograms. A Ge/KBr beamsplitter was used to cover the spectral region, and a DTGS detector was chosen because of its linear response. Background spectra of the empty gas cell were recorded before and after each sample spectrum to check for baseline drift. The sample (company etc, I got it from NILU) was degassed under vacuum at 40 °C to remove water, ammonia and other possible volatile impurities. Spectra were obtained of the vapours in equilibrium above a thermostatted sample at 4 different temperatures between 12 and 27 °C ($\delta T = \pm 0.5$ K).

The absolute infrared absorption cross section of gaseous MEA was obtained from the FT-IR spectra using the OH stretching band region of MEA (3510-3800 cm^{-1}) for the calibration. The integrated cross-section of the OH stretching band region was determined by plotting the integrated absorbance intensities against the product of the number density and pathlength. Conservative estimates of systematic errors are: sample pressure (<5 %), path length (<1 %), temperature (<1 %), and definition of the baseline in the integration procedure (<5 %). The estimated accuracy of the absolute absorption cross section is believed to be better than ± 7 % including possible baseline offset. Retrieval of chemical components from the FT-IR spectra is sensitive to detector non-linearity and interference of compounds with overlapping spectra. For compounds whose spectra only show *PQR*-structure the retrieval procedure has an estimated uncertainty of ±10 %. For compounds showing rotational fine structure the retrieval procedure has an estimated uncertainty of ±5 %.

2.3 EUPHORE chamber studies

A series of photo-oxidation experiments were carried out at the European Photochemical Reactor, EUPHORE, in Valencia, Spain (longitude –0.5, latitude 39.5). The EUPHORE reactor is an "open access" large scale facility established in 1991 as part of the CEAM Centre of Applied Research with financial support from EU, http://www.ceam.es/html/index_i.htm. There are two ~200 m^3 hemispherical chambers for photochemical studies. The chambers are constructed from Teflon film, which have a uniform transmission of sunlight, and are protected by steel canopies which are opened during the photo-oxidation experiments. After the experiments the chambers are closed and flushed overnight with scrubbed air. The floors of the chambers are cooled to ensure a stable temperature in the chambers during the experiments.

The EUPHORE facility offers a long range of analytical instrumentation for on-line detection of chemical components and particles in the chamber (FT-IR, GC-MS, SMPS, TEOM, and monitors for actinix flux, CH_2O, NO_x, NO_y, CO, H_2O, O_3, HONO). A detailed description of the EUPHORE facility and the existing analytical instruments is available in the literature.[24-28]

To complement the in-house instrumentation, users may attach own instrumentation and sample collection. The ADA project provided two additional on-line instruments: an Aerosol Mass Spectrometer (AMS) and a High-Resolution Proton-Transfer-Reaction Time-of-Flight Mass Spectrometer (PTR-TOF-MS). The high mass resolution of this instrument allows an (almost) unambiguous determination of the sum formulae of ions detected – structural isomers exempt. In addition, reactor air was sampled 3 times a day employing various adsorbents for subsequent analysis at NILU (amines, nitrosamines, nitramines, carbonyls, VOC).

Two experiment campaigns were conducted. The first campaign took place in May 2009 and included the additional PTR-TOF-MS and AMS instruments. The planned experiments in this campaign included:

1. Photo-oxidation in dry air and under low-NOx conditions
2. Photo-oxidation in dry air and under various high-NOx conditions
3. Photo-oxidation in dry air under high-NOx and dark conditions
4. Photo-oxidation in 20% RH air and under low-NOx conditions
5. Photo-oxidation in 20% RH air and under various high-NOx conditions
6. Photo-oxidation of $NH_2CD_2CH_2OH$ in dry air and low-NOx conditions
7. Photo-oxidation of $NH_2CH_2CD_2OH$ in dry air and low-NOx conditions
8. Photo-oxidation of $NH_2CD_2CD_2OH$ in dry air and low-NOx conditions
9. Photo-oxidation of $ONNHCH_2CH_2OH$ under high-NOx conditions
10. Long time oxidation in 20% RH air and under high-NOx conditions with inorganic aerosol particles present

It was not possible to synthesise the nitrosamine, $ONNHCH_2CH_2OH$, and experiment (8) was therefore not carried out. Further, the "20 % Relative Humidity experiments" had to be abandoned because the increased humidity resulted in such fast removal of MEA from the vapour phase that photo-chemical

experiments became futile. Instead, other experiments from the list were repeated under various different conditions.

The September campaign included:

11. Photo-oxidation of $CH_3CH_2NH_2$ under high-NOx conditions in dry air.
12. Photo-oxidation of MEA in dry air under high-NO_x conditions.
13. Photo-oxidation of MEA in dry air under low-NO_x conditions.
14. Photo-oxidation of MEA in dry air under dark, high-NO_x conditions.

A typical EUPHORE experiment started around 06:00 UT when reagents were added to the chamber. The canopy of the chamber was opened after the reagents were considered to be well-mixed, and the first air samples had been collected. The MEA experiments lasted up to 12 hours after which the chamber was closed, a high-volume collection of aerosol carried out, and then flushed overnight with scrubbed air.

Unlike the typical laboratory smog chamber, purified air is constantly added to compensate for leakage, loss through connections, sampling on filters and continuous sampling by ozone, NO_x and other monitors. This is corrected for in the data analysis: SF_6 and CH_3CN were added in order to measure the apparent dilution rate by FT-IR and PTR-TOF-MS, respectively.

The following experiments have been carried out:

No.	Date	Instruments[a]	Comments
1	2009.05.06	A, P, F, O, S	Instrument tests
2	2009.05.07	A, P, F, O, S	Low-NO_x experiment, dry conditions with HONO as OH precursor. Extensive particle formation, experiment discarded.
3	2009.05.08	A, P, F, O, S	Low-NO_x experiment, dry conditions with H_2O_2 as OH precursor. The NO contained HNO_3 leading to extensive particle formation. Experiment discarded.
4	2009.05.09	A, P, F, O, S	Low-NO_x experiment, dry conditions with H_2O_2 as OH precursor. Reaction between H_2O_2 and MEA. Experiment discarded.
5	2009.05.10	A, P, F, O, S	High-NO_x experiment, dry conditions. Low MEA concentration.
6	2009.05.11	A, P, F, O, S	High-NO_x experiment, dry conditions.
7	2009.05.12	A, P, F, O, S	High-NO_x experiment, humid conditions. Rapid loss of MEA to the walls. Experiment discarded.
8	2009.05.13	A, P, F, O, S	Dark chemistry experiment. Rapid MEA loss during addition of O_3 and extensive particle formation. Experiment discarded.
9	2009.05.14	A, P, F, O, S	High-NO_x experiment, dry conditions
10	2009.05.15	A, P, F, O, S	Low-NO_x, seeding aerosol experiment (~100 µg/m3).
11	2009.05.18	A, P, F, O, S	$H_2NCD_2CD_2OH$: Conditioning the chamber. High-NO_x experiment, dry conditions.

			Extensive wall exchange of isotopologues. Experiment discarded.
12	2009.05.19	A, P, F, O	$H_2NCD_2CD_2OH$:. Low-NO_x experiment, dry conditions.
13	2009.05.20	A, P, F, O	$H_2NCH_2CD_2OH$: Conditioning the chamber. Extensive wall exchange of isotopologues. Experiment discarded.
14	2009.05.21	P, F, O	$H_2NCH_2CD_2OH$: High-NO_x experiment, dry conditions.
	2009.05.22		Conditioning the chamber for experiments with $H_2NCD_2CH_2OH$.
15	2009.05.25	P, F, O	$H_2NCD_2CH_2OH$: High-NO_x experiment, dry conditions. . Extensive wall exchange of isotopologues. Experiment discarded.
16	2009.05.26	P, F, O	$H_2NCD_2CH_2OH$: High-NO_x experiment, dry conditions.
17	2009.05.27	P, F, O	CH_3NH_2: High-NOx experiment, dry conditions.
19	2009.09.03	F, O	$CH_3CH_2NH_2$ high-NO_x experiment, dry conditions. Ethylamine removed rapidly from gas phase. Extensive particle formation, experiment discarded.
20	2009.09.07	F, O	LOPAP (HONO) monitor identified as HCl-source causing extensive particle formation and fast amine removal from gas phase. Experiment discarded.
21	2009.09.08	F, O	$CH_3CH_2NH_2$ high-NOx experiment, dry conditions.
22	2009.09.09	F, O	MEA high-NOx experiment with seeding particles. Extensive wall exchange of gas phase MEA with $CH_3CH_2NH_2$ release to the gas phase. Experiment discarded.
23	2009.09.10	F, O	MEA high-NO_x experiment, dry conditions. High MEA concentration.
24	2009.09.11	F, O	MEA low-NO_x experiment, dry conditions. High MEA concentration.
25	2009.05.13	F, O	MEA high-NO_x, dark experiment, dry conditions. (Heavy rainfall)

[a] A, Aerosol Mass Spectrometer (AMS); P, Proton Transfer Reaction – Time of Flight - Mass Spectrometry (PTR-TOF-MS); F, Fourier Transform Infrared (FT-IR); O, sampling for Off-line analysis; S, Scanning Mobility Particle Sizer (SMPS).

The present report includes results from experiments 5, 6, 9, 10, 12 and 23. Experiments 5, 6, 9 and 10 have been analysed in detail by a chamber chemistry and aerosol formation model to achieve mass balance and branching ratios.

2.4 Results from the EUPHORE chamber studies

2.4.1 Interpretation of the experiments

Figure 2.2 illustrates a typical time series of data produced by the PTR-TOF-MS instrument. The figure shows the time evolution of MEA and the inert dilution tracer (acetonitrile, CH_3CN) in the EUPHORE chamber during the photo-oxidation experiment on May 10. Additional information about opening and closing times of the chamber canopy and the time span selected for a more detailed analysis is also displayed. The peak volume mixing ratio in the experiment was around 130 ppbV which corresponds to about 60 mg gas phase MEA in the chamber. For comparison the *in situ* FT-IR data showed 125 ppbV as the average mixing ratio during sampling period 1, see Figure 2.2. Results from off-line analysis of filter samples gave significantly higher average values than the on-line and *in situ* FT-IR observations: $<[MEA]>_1 = 390$ ppbV, $<[MEA]>_2 = 300$ ppbV, and $<[MEA]>_3 = 160$ ppbV.
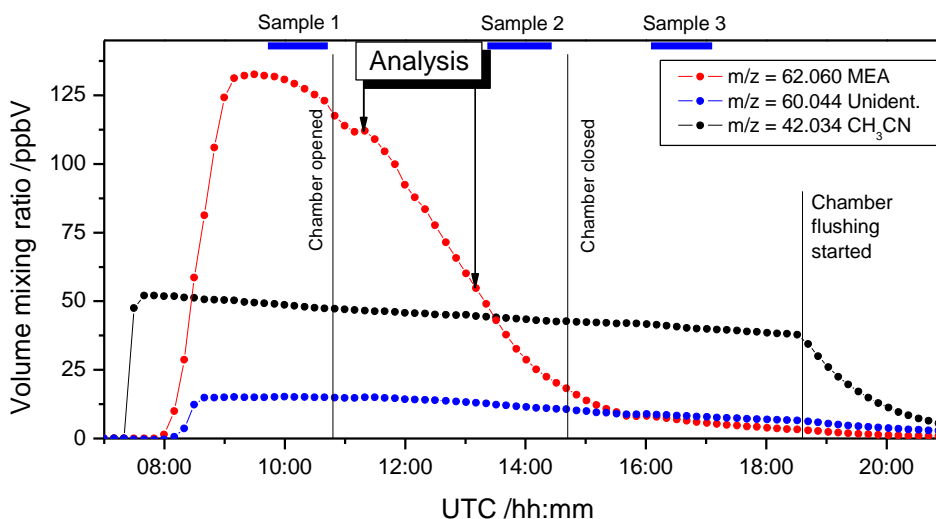
Figure 2.2. Time evolution of MEA (m/z 62.060), acetonitrile (m/z 42.034) and an impurity in the administered MEA sample (m/z 60.044), as measured by PTR-TOF-MS. Off-line sampling periods are indicated on top of frame. Data from the experiment on May 10, 2009.

An analysis of the dilution tracer yields a dilution rate constant $k_{dil} = 8.1 \times 10^{-6}$ s^{-1} in this particular experiment. This corresponds to a dilution loss of around 6 % in 2 hours, which contrasts the observed 51 % loss of MEA in the same time span. Other loss processes (wall loss and aerosol formation) will be discussed later.

The PTR-TOF-MS instrument detected an additional ion signal at m/z 60.044 which corresponds to an ion with the sum formula: $C_2H_6NO^+$. Under the assumption that this ion corresponds to a protonated parent molecule potential neutral precursors are: NH_2CH_2CHO (amino acetaldehyde, CAS: 6542-88-7), $NH_2C(O)CH_3$ (acetamide, CAS: 60-35-5), CH_3NHCHO (*N*-methyl formamide, CAS: 123-39-7), c(-NH-O-CH$_2$-CH$_2$-) (1,2-oxazetidine, CAS: 287-33-2), $HN=CHCH_2OH$ (2-imino ethanol, CAS:724427-16-1(Z), CAS:7244-18-3(E)), or c(-O-CH$_2$-CH-)NH$_2$ (2-oxiranamine, CAS: 54160-59-7). Analyses of the Tenax TA adsorption tube and the DNPH cartridge collected <u>before</u> the opening of the chamber canopy

revealed no traces of the more obvious candidate NH_2CH_2CHO (and no traces of other species with the correct mass).

The m/z 60.044 signal is included in Figure 2.2 and displays a quite different time profile than the MEA signal. It is clear from the figure that the unidentified compound is orders of magnitude less reactive than MEA which rules out amino acetaldehyde, NH_2CH_2CHO, and 2-imino ethanol, $HN=CHCH_2OH$.

Figure 2.3 summarises the differences between the PTR-TOF-MS spectra obtained at the end and at the beginning of the time frame "Analysis" indicated in Figure 2.2. The signals have been normalized to the loss in the major MEA signal at m/z 62.060.
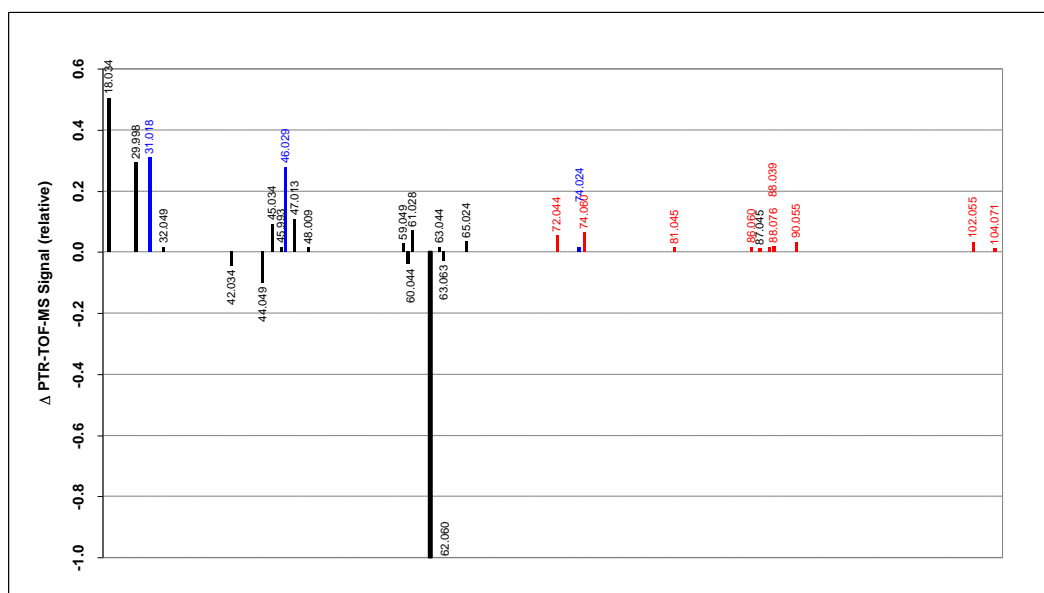
Figure 2.3. Normalized difference in mass spectra measured during the photo-oxidation of MEA on May 10, 2009. Signals smaller than 1% of $\Delta I_{62.060}$ (MEA) have been omitted.

Only three other ions were detected with masses corresponding exactly to those of theoretically predicted products (highlighted in blue in Figure 2.3 and Table 2.1). The ion at m/z 31.018 corresponds to protonated formaldehyde, the ion with m/z 46.029 is assigned to protonated formamide, and the ion at m/z 74.024 may be tentatively assigned to protonated 2-oxo acetamide ($NH_2C(O)CHO$, CAS: 60939-21-1). The time evolution of the latter two (magnified) ion signals are included in Figure 2.4 from which it can be seen that the two signals do not correlate well during the photolysis period: the m/z 74.024 ion signal is clearly delayed relative to the m/z 46.029 ion signal and continues to grow in the dark/dusk when the chamber canopy is closed. The latter signal is due to formamide and is a primary photo-oxidation product, while the former must, at least in part, be a secondary photo-oxidation product.

Table 2.1. Observed ion signals larger than 1% of $\Delta I_{62.060}$ (MEA) in mass spectra measured at start and end of the analysis time span during the photo-oxidation of MEA on May 10, 2009.

m/z	Ion formula	Off-line confirmation	Potential neutral precursor	Comments
18.034	H_4N		Ammonia aminoacetaldehyde 2-imino ethanol	surface chemistry (?) ion chemistry (?) ion chemistry (?)
29.998	NO		nitrogen dioxide	HONO formation[1]
31.018	CH_3O	DNPH-method	formaldehyde	partly chamber artefact[2]
32.049	CH_6N	Filter-method	methylamine	artefact[3]
42.034	C_2H_4N	Tenax-method	acetonitrile	dilution tracer
44.049	C_2H_6N		MEA	$[MH^+\text{-}H_2O]$
45.034	C_2H_5O	Tenax-method DNPH-method	acetaldehyde oxirane ethylene glycol	partly chamber artefact[1] surface chemistry $[MH^+\text{-}H_2O]$, surface chem.
45.993	NO_2		nitric acid	$NO_2+OH \rightarrow HNO_3$
46.029	CH_4NO	Tenax-method	formamide	
47.013	CH_3O_2	Tenax-method	formic acid	chamber artefact[2]
48.009	H_2O_2N		nitrogen dioxide	HONO formation[1]
59.049	C_3H_7O	DNPH-method	acetone	chamber artefact[2]
60.044	C_2H_6NO	DNPH-method Tenax-method	amino acetaldehyde acetamide 2-imino ethanol	
61.028	$C_2H_5O_2$	DNPH-method Tenax-method	glycolaldehyde acetic acid	surface chemistry chamber artefact[2]
62.060	C_2H_8NO	Filter-method	MEA	
63.044	$C_2H_7O_2$	Tenax-method	ethylene glycol	surface chemistry
63.063	$^{13}CCH_8NO$	Filter-method	MEA	^{13}C-MEA
65.024	CH_5O_3		formic acid	$[MH^++H_2O]$ chamber artefact[2]
72.044	C_3H_6NO	Tenax-method	4,5-dihydrooxazole (or isomer)	condensation product
74.024	$C_2H_4NO_2$	DNPH-method	2-oxo-acetamide (or isomer)	
74.060	C_3H_8NO			condensation product
81.045	$C_4H_5N_2$	Tenax-method	Pyrazine (or isomer)	condensation product
86.060	C_4H_8NO	Tenax-method	4,5-dihydro-2-methyloxazole (or isomer)	condensation product
87.045	$C_4H_7O_2$			
88.039	$C_3H_6NO_2$	Tenax-method	2-oxazolidone (or isomer)	condensation product
88.076	$C_4H_{10}NO$			condensation product
90.055	$C_3H_8NO_2$			condensation product
102.055	$C_4H_8NO_2$			condensation product
104.071	$C_4H_{10}NO_2$	Tenax-method	N-acetylethanolamine (or isomer)	condensation product

[1] 2 NO_2 (gas) + H_2O (surface) $\rightarrow$ HNO_2 (gas) + HNO_3 (surface); H_3O^+ + HNO_2 $\rightarrow$ $H_2O_2N^+$ + H_2O; H_3O^+ + HNO_2 $\rightarrow$ NO^+ + H_2O + H_2O. [2] Chamber artefact: a product that is also observed when the clean chamber (filled with zero air only) is exposed to sunlight. [3] Artefact from a previous experiment; not seen during later experiments
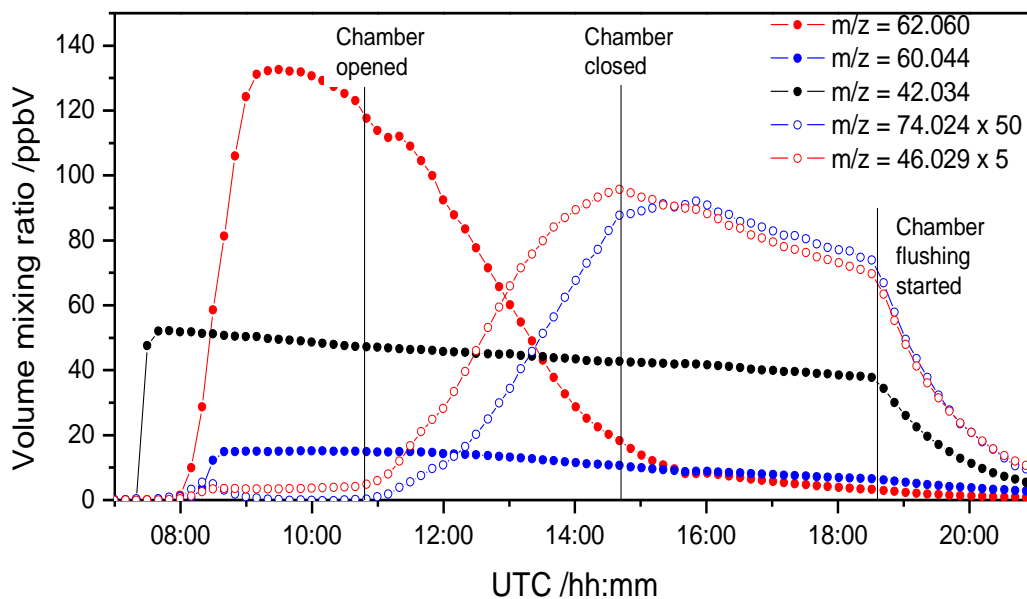
Figure 2.4. Time evolution of MEA (m/z 62.060), acetonitrile (m/z 42.034), "unidentified" (m/z 60.044), and the two products formamide (m/z = 46.029, 5 times enhanced) and 2-oxo acetamide (m/z = 74.024, 50 times enhanced) as measured by PTR-TOF-MS. Data from the experiment on May 10, 2009.

Nine of the observed product ion signals stem, unexpectedly, from N-containing C_3 and C_4 compounds. These signals are highlighted in red in Figure 2.3 and Table 2.1 and are explained by condensation reactions between aldehydes, ketones, carboxylic acids and imines on chamber and instrument inlet surfaces. A recent *in situ* study demonstrates a fast surface-catalyzed reaction between 2,2-dimethylpropanal and methanamine,[29] and a similar observation of products with more carbon atoms than the reactant was also made by Pitts *et al.* in their photo-oxidation study of diethylamine.[11]
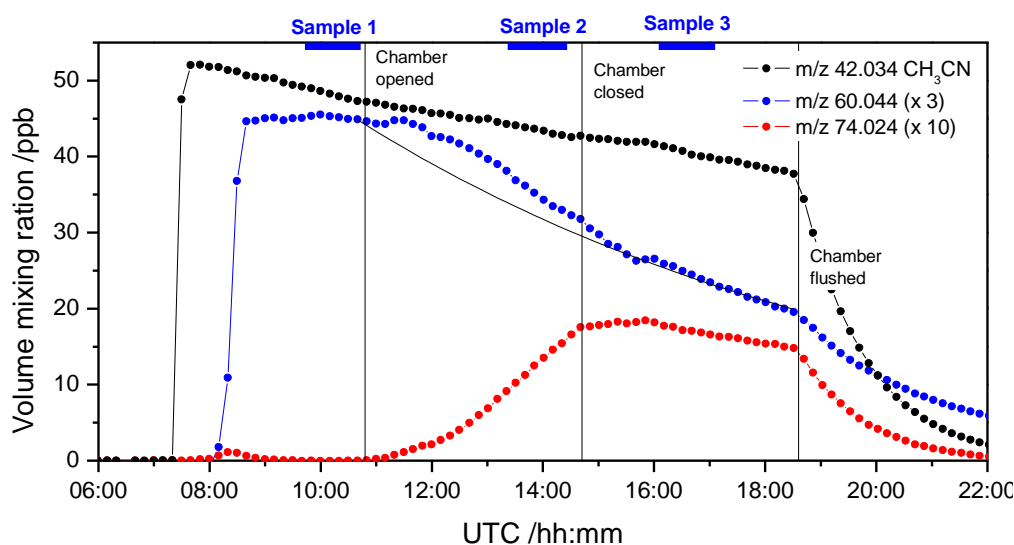
Figure 2.5. Time evolution of the m/z 60.044 (unidentified), m/z 74.024 (2-oxo acetamide) and mz/ 42.034 (CH_3CN) ion signals during the photo-oxidation experiment on May 10, 2009. Periods of sampling for off-line analysis are indicated on top of frame. The solid curve represents an exponential decay of the m/z 60.044 ion signal fitted to the observed decay after closing the chamber canopy.

A closer inspection of the m/z 60.044 ion signal reveals a production term during the time period when the chamber canopy was open (see Figure 2.5). This becomes very clear when the signal is compared to an exponential loss function, τ_{loss} ~7 h, fitted to the m/z 60.044 signal observed after closing the chamber canopy. In experiments with higher starting concentrations of MEA the initial m/z 60.044 ion signal does not increase in proportion. However, the *additional* m/z 60.044 ion signal becomes correspondingly larger during the photo-oxidation of MEA.

The observations suggest that: (1) the m/z 60.044 ion signal origins in several structural isomers, (2) one or more of these isomers is formed during the photo-oxidation experiment, and (3) one or more of the structural isomers produced in the photo-oxidation of MEA undergo further reactions in the time period the chamber canopy is open. Figure 2.6 illustrates an apparent kinetic relationship between the additional m/z 60.044 ion signal produced during photo-oxidation of MEA (obtained by subtracting the "background" described above from the total m/z 60.044 ion signal) and the m/z 74.024 ion signal. In spite of high uncertainty in extracting the intermediate C_2H_5ON-isomer m/z 60.044 signal, the figure shows the relatively short lifetime of the compound, and the apparently near quantitative photo-oxidation to $C_2H_3O_2N$ (2-oxo acetamide). This suggests that the additional m/z 60.044 signal may stem from amino acetaldehyde (AAA). However, the results from off-line analysis of DNPH cartridges do not support this hypothesis: $<AAA>_1$ <0.02 ppbV, $<AAA>_2$ = 0.03 ppbV, and $<AAA>_3$ = 0.04 ppbV. The DNPH quantification of amino acetaldehyde is more uncertain than for other carbonyls reported because the reference compound is not available (amino acetaldehyde polymerises as soon as formed in the liquid). However, we may still deduce that the additional m/z 60.044 ion signal observed by PTR-TOF-MS does not originate in amino acetaldehyde alone.
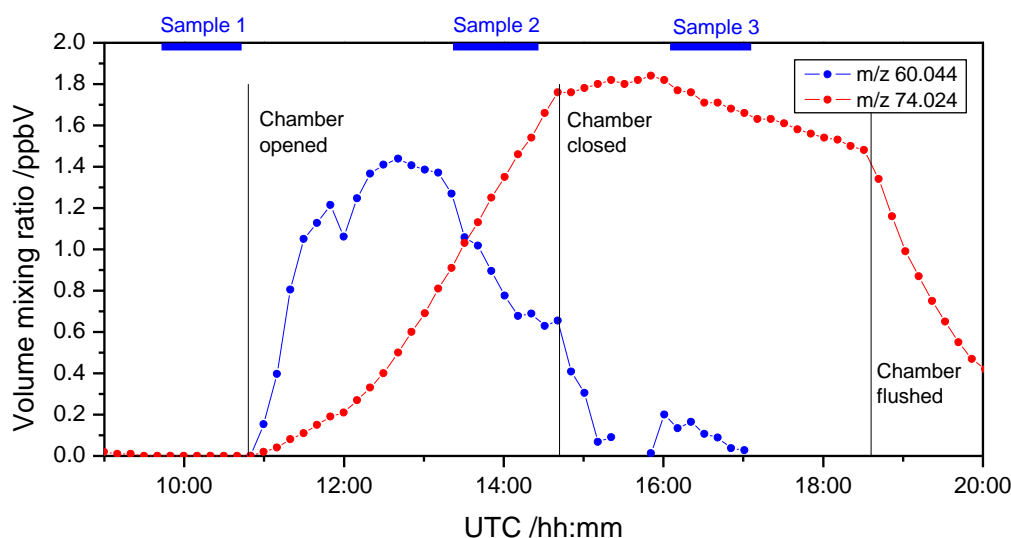
Figure 2.6. Time evolution of the additional m/z 60.044 ion signal produced during photo-oxidation of MEA (see text for details) and the m/z 74.024 ion signal of 2-oxo acetamide. Off-line sampling periods are indicated on top of frame. Data from the photo-oxidation experiment on May 10, 2009.

Figure 2.7 displays the ion signals from MEA, the dilution tracer, 2-oxo acetamide (m/z 74.024), and the m/z 60.044 ion signal from the experiment on May 15 in which the initial MEA volume mixing ratio was around 7 times larger than in the May 10 experiment. The intermediate product signal at m/z 60.044 is now obvious on top of the "background" and it amounts to around 5 ppbV at its peak. The results from off-line analysis of DNPH cartridges from this experiment again indicate that the additional ion signal cannot originate from amino acetaldehyde (AAA): $<AAA>_1 < 0.01$ ppbV, $<AAA>_2 = 0.02$ ppbV, and $<AAA>_3 = 0.03$ ppbV. Furthermore, the increase in the ion signal corresponding to 2-oxo acetamide is now obviously not correlated to the additional m/z 60.044 signal.
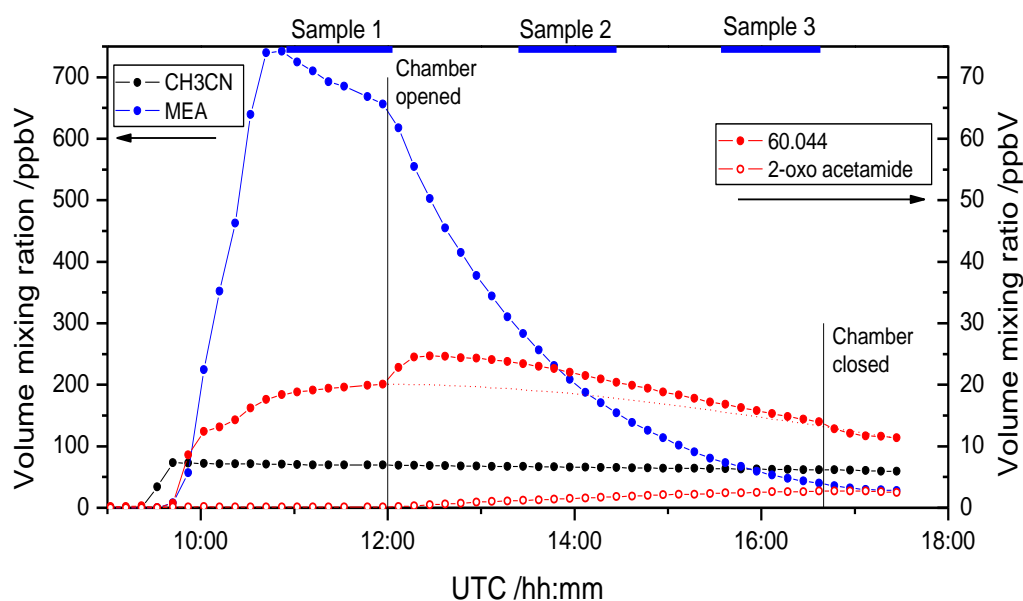
Figure 2.7. Time evolution of the m/z 62.060 (MEA), m/z, m/z 42.034 (CH_3CN), m/z 60.044 (partly NH_2CH_2CHO) and m/z 74.024 ($NH_2C(O)CHO$) ion signals during the photo-oxidation experiment on May 15, 2009. Off-line sampling periods are indicated on top of frame.

It is clear that the *additional* m/z 60.044 signal is related to the photo-oxidation of MEA, and the only alternative is the structural isomer $HN=CHCH_2OH$, which is an expected intermediate product following hydrogen abstraction from the amino group, see Scheme 1.3.

The signal at m/z 31.018 is, as mentioned above, assigned to protonated formaldehyde, the m/z signal at 45.034 ($C_2H_5O^+$) is assigned to protonated acetaldehyde (CAS: 75-07-0) or protonated oxirane (ethylene oxide, CAS: 75-21-08) or protonated ethylene glycol which primarily dehydrates upon protonation, see later. The m/z signal at 61.028 ($C_2H_5O_2^+$) is assigned to protonated glycolaldehyde (hydroxyl acetaldehyde, CAS: 141-46-8). This ion may be formed from protonation of neutral glycolaldehyde or via the reaction of H_3O^+ with amino acetaldehyde or 2-imino ethanol (see later). The m/z 61.028 signal may in principle also originate from protonation of acetic acid which is commonly formed in smog chambers as an artefact. However, protonated acetic acid partly dehydrates in the PTR-TOF-MS to form the CH_3CO^+ ion which is barely observed. Small aldehydes are commonly formed as artefacts during chamber photo-oxidation studies, but the observed levels (in particular formaldehyde) exceed

typical artefact levels. Figure 2.8 compares the results for formaldehyde obtained from on-line PTR-TOF-MS, *in situ* FT-IR and off-line analysis of DNPH-cartridges. The FT-IR results were obtained from an analysis of the v_1 (A_1) ro-vibrational bands employing line-strengths from the HITRAN data base.[23] It can be seen that the FT-IR data (uncertainty ± 3 ppbV) agree well with the DNPH-cartridge results, and that the PTR-TOF-MS data are almost a factor of two larger. However, formaldehyde is difficult to quantify by PTR-TOF-MS and the m/z 31.018 ion may also have other precursors.
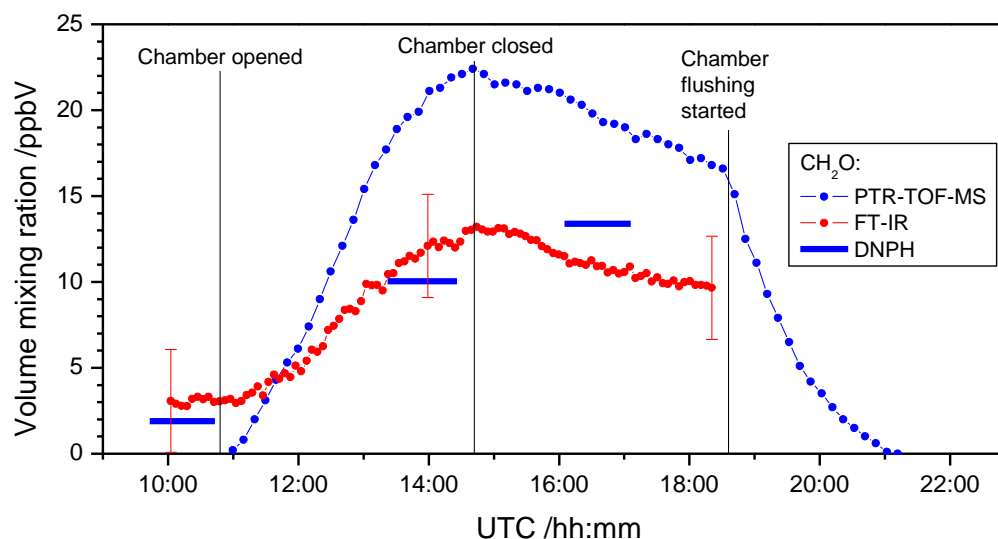
Figure 2.8. Time evolution of formaldehyde as measured by on-line PTR-TOF-MS (m/z 31.018), *in situ* FT-IR and off-lien analysis of DNPH cartridges during the photo-oxidation experiment on May 10, 2009. Error bars (FT-IR) defined by S/N = 2.

The m/z signals at 45.034 and 61.028 are, as mentioned above, tentatively assigned to protonated acetaldehyde and/or oxirane and/or dehydrated protonated ethylene glycol, and to protonated glycolaldehyde (stemming from different neutral precursors), respectively. The time evolution of the two ion signals are displayed in Figure 2.9. The off-line analysis of DNPH cartridges show the presence of acetaldehyde (AA) in amounts agreeing with the PTR-TOF-MS results: $<[AA]>_1 = 0.17$ ppbV, $<[AA]>_2 = 7.37$ ppbV, $<[AA]>_3 = 6.98$ ppbV, Figure 2.9. The DNPH cartridges also showed the presence of glycolaldehyde (GA): $<[GA]>_1 = <0.1$ ppbV, $<[GA]>_2 = 1.73$ ppbV, $<[GA]>_3 = 2.02$ ppbV. The corresponding ($C_2HD_4O^+$ and $C_2H_2D_3O_2^+$) ion signals were observed during the MEA-d_4 photo-oxidation experiments which implies that the compounds all have their origin in the administered MEA sample. Acetaldehyde and acetic acid, however, cannot possibly be formed from MEA as this requires the formation of an additional C-H bond to give a CH_3-group. On the other hand, MEA is produced by reaction of oxirane with ammonia and the reverse reaction may easily be envisaged to occur on surfaces under solar radiation: $NH_2CH_2CH_2OH \rightarrow$ c(-CH_2CH_2O-) + NH_3. Concerted hydrolysis or subsequent hydrolysis of oxirane on the Teflon surfaces will result in the formation of ethylene glycol, CH_2OHCH_2OH, which has a high surface affinity, and which therefore will not enter the vapour phase to a large extent. The small m/z 63.044 ion signal corresponds to $C_2H_7O_2^+$, the sum formula of protonated ethylene glycol. In the PTR-TOF-MS reaction

chamber, around 90 % of protonated ethylene glycol dehydrates to form a $C_2H_5O^+$ ion, $C_2H_7O_2^+ \rightarrow C_2H_5O^+ + H_2O$, and the major ion signal from ethylene glycol therefore coincides with those of protonated acetaldehyde and protonated oxirane. Ethylene glycol may also undergo oxidation in the gas phase, or oxidation on the Teflon surfaces similar to aqueous phase reactions,[30] which in both cases results in the formation of glycolaldehyde, CH_2OHCHO. We note that small amounts of ethylene glycol are found on Tenax samples collected before opening the canopy.
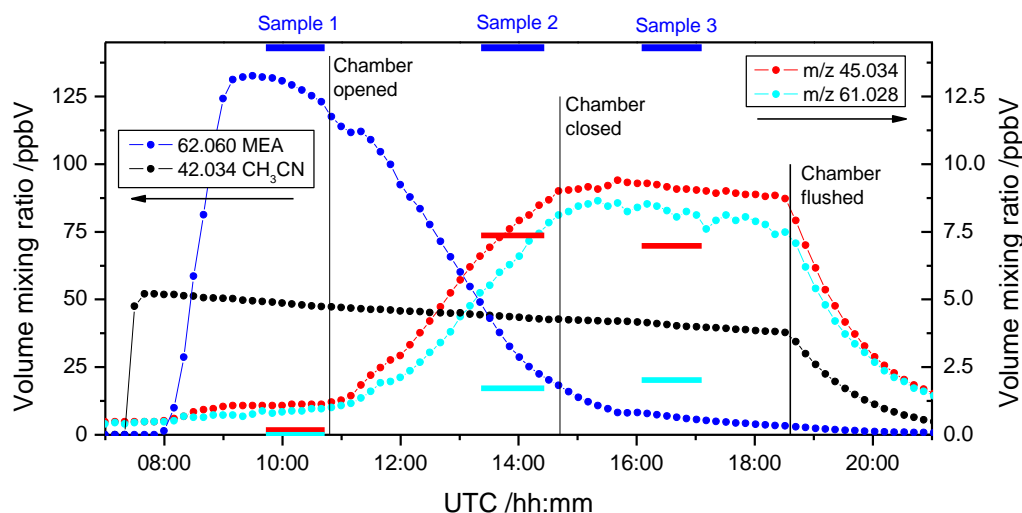
Figure 2.9. Time evolution of MEA, CH_3CN, m/z 45.034 (acetaldehyde and/or oxirane and/or dehydrated ethylene glycol) and m/z 61.028 (glycolaldehyde and/or acetic acid) as measured by on-line PTR-TOF-MS during the photo-oxidation experiment on May 10, 2009. The results from off-line analysis of DNPH cartridges are included for comparison; acetaldehyde (red) and glycolaldehyde (cyan).

The importance of MEA wall adsorption and desorption is illustrated in Figure 2.10 which shows the time profiles of MEA and MEA-d_4 ($NH_2CD_2CD_2OH$) during the experiment on May 19 – the second day of experiments with MEA-d_4 after several days of experiments with MEA. The isotopic purity of MEA-d_4 was > 99%
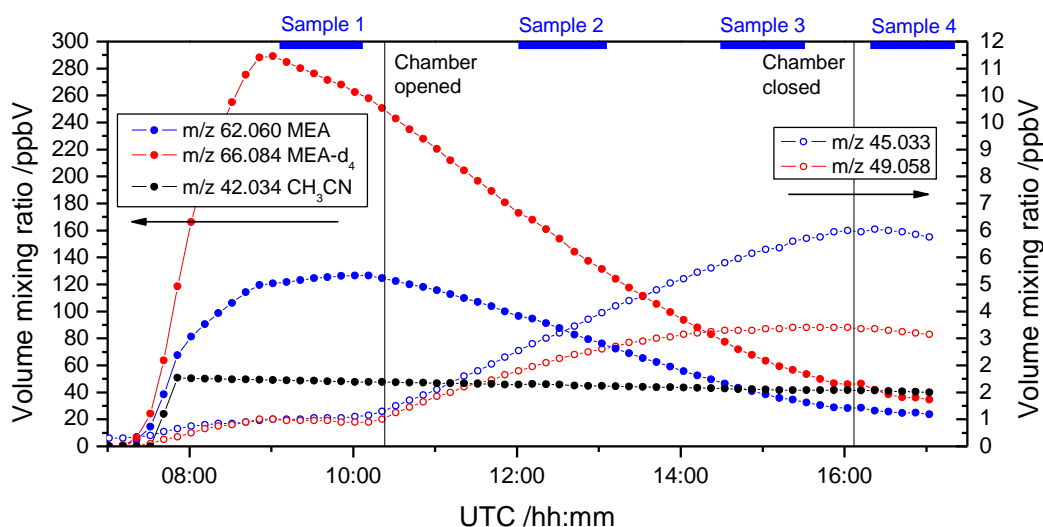
Figure 2.10. Time evolution of the m/z 62.060 (MEA), m/z 66.084 (MEA-d_4), m/z 42.034 (CH_3CN), m/z 45.033 (C_2H_4O) and m/z 49.058 (C_2D_4O) signals during the photo-oxidation experiment on May 19, 2009. Periods of sampling for off-line analysis are indicated on top of the frame.

and the appearance of MEA in the chamber (also observed by *in situ* FT-IR) upon administering MEA-d_4 shows that a substantial amount of MEA was adsorbed on the chamber walls (with a total surface area of around 200 m^2 and a site area of 10×10 Å molecule^{-1}, 3 mono-layers on the chamber surfaces corresponds to ca. 130 ppbV in the gas phase). It is obvious from Figure 2.10 that MEA-d_4 is removed faster from the gas phase than MEA throughout the experiment. This is explained by the dynamic chamber wall adsorption/desorption of MEA-d_4 in competition with MEA in addition to particle formation and the photo-oxidation by OH radicals.

Figure 2.10 includes the ion signals m/z 45.033 ($C_2H_5O^+$) and 49.058 ($C_2HD_4O^+$) originating from respectively parent and deuterated acetaldehyde/oxirane/ ethylene glycol. It can be seen that the $C_2H_5O^+$ signal is larger than the $C_2HD_4O^+$ signal in contrast to there being more MEA-d_4 than MEA in the gas phase. Since the barrier to shifting a hydrogen from one carbon atom to another is too high to take place at room temperature, even in catalyzed processes, this suggests that the $C_2H_5O^+$ signal origins in acetaldehyde/oxirane/ethylene glycol while the $C_2HD_4O^+$ signal only originates in deuterated oxirane/ethylene glycol. This is also supported by the observed ratio between the m/z 45.033 ($C_2H_5O^+$) and 49.058 ($C_2HD_4O^+$) ion signals which increases with time from around 1 at 9 UTC to 1.8 at 16 UTC. The off-line analysis of DNPH cartridges collected on May 19 gave the following total acetaldehyde (AA) mixing ratios: $<[AA]>_1 = 0.31$ ppbV, $<[AA]>_2 = 5.52$ ppbV, $<[AA]>_3 = 12.13$ ppbV and $<[AA]>_4 = 12.31$ ppbV. The results from the off-line analysis of the isotopic composition of acetaldehyde is summarized in Table 2.2. The analysis of the DNPH cartridges from the isotope experiment confirms that the detected acetaldehyde-d_0 does not stem from MEA and that the PTR-TOF-MS m/z 49.058 ($C_2HD_4O^+$) ion signal only originates in deuterated oxirane/ethylene glycol. We offer no additional interpretation of the acetaldehyde isotopic composition.

Table 2.2. Isotopic composition (/µg m^{-3}) of acetaldehyde during the photo-oxidation experiment on May 19, 2009. Volume mixing ratios (/ppbV) are given in parentheses.

Isotopologue	D0	D1	D2	D3	D4
Sample 1	0.30 (0.17)	0.01 (0.00)			
Sample 2	3.97 (2.22)	1.03 (0.57)	0.24 (0.13)	0.16 (0.08)	0.12 (0.06)
Sample 3	9.12 (5.10)	1.82 (1.00)	0.55 (0.29)	0.36 (0.19)	0.27 (0.14)
Sample 4	9.26 (5.18)	1.67 (0.91)	0.65 (0.35)	0.46 (0.24)	0.28 (0.14)

The time evolution and relative intensities of the PTR-TOF-MS m/z 61.029 ($C_2H_5O_2^+$) and 64.047 ($C_2HD_4O_2^+$) ion signals resemble those of m/z 45.033 ($C_2H_5O^+$) and 49.058 ($C_2HD_4O^+$) shown in Figure 2.10; the $C_2H_5O_2^+$ signal is at all times larger than that of $C_2HD_4O_2^+$. The ratio between the m/z 61.029 ($C_2H_5O_2^+$) and 64.047 ($C_2HD_4O_2^+$) ion signals first decreases with time from around 3.5 at 10:23 UTC to around 2.3 at 11 UTC, then the ratio increases with time to around 3.8 at 16 UTC. The off-line analysis of DNPH cartridges collected on May 19 gave the following total glycolaldehyde (GA) mixing ratios: $<[AA]>_1 = 0.36$ ppbV, $<[AA]>_2 = 2.30$ ppbV, $<[AA]>_3 = 5.18$ ppbV and $<[AA]>_4 = 6.81$ ppbV. The results

from the off-line analysis of the isotopic composition of glycol aldehyde is summarized in Table 2.3.

Table 2.3. Isotopic composition (/μg m^{-3}) of glycolaldehyde during the photo-oxidation experiment on May 19, 2009. Volume mixing ratios (/ppbV) are given in parentheses.				
Isotopologue	D0	D1	D2	D3	D4
Sample 1	0.03 (0.01)		0.11 (0.04)	0.75 (0.29)	
Sample 2	2.37 (0.97)		0.20 (0.08)	2.79 (1.09)	0.25 (0.10)
Sample 3	6.10 (2.50)		0.67 (0.27)	5.12 (2.00)	0.73 (0.28)
Sample 4	7.98 (3.28)		1.12 (0.44)	6.79 (2.65)	0.72 (0.28)

The isotopic composition of glycolaldehyde, Table 2.3, contrasts that of acet-aldehyde, Table 2.2, and confirms that the observed glycolaldehyde originates from MEA.

Figure 2.11 displays the time evolution of the main photo-oxidation product NH_2CHO (from the photo-oxidation of MEA) and NH_2CDO (from the photo-oxidation of MEA-d_4). It can be seen that less C-deutero formamide (NH_2CDO) than parent formamide (NH_2CHO) is formed during the experiment in spite of [MEA-d_4] > [MEA]. This reflects the kinetic isotope effect in the initial C-H/C-D abstraction reaction by OH radicals. The figure also includes the results from off-line analysis of Tenax TA adsorption tubes which confirms the isotopic composition of formamide in the experiment. The mixing ratios of CH_2O and CD_2O are around 3:2 during the experiment and compare well with the formamide isotopologue mixing ratios. This may, in part, be coincidental because *i)* formaldehyde reacts much faster with OH than formamide does, and *ii)* there are also isotope effects in the formaldehyde/OH reaction[31-32] and in the formaldehyde photolysis frequency.[33-34]
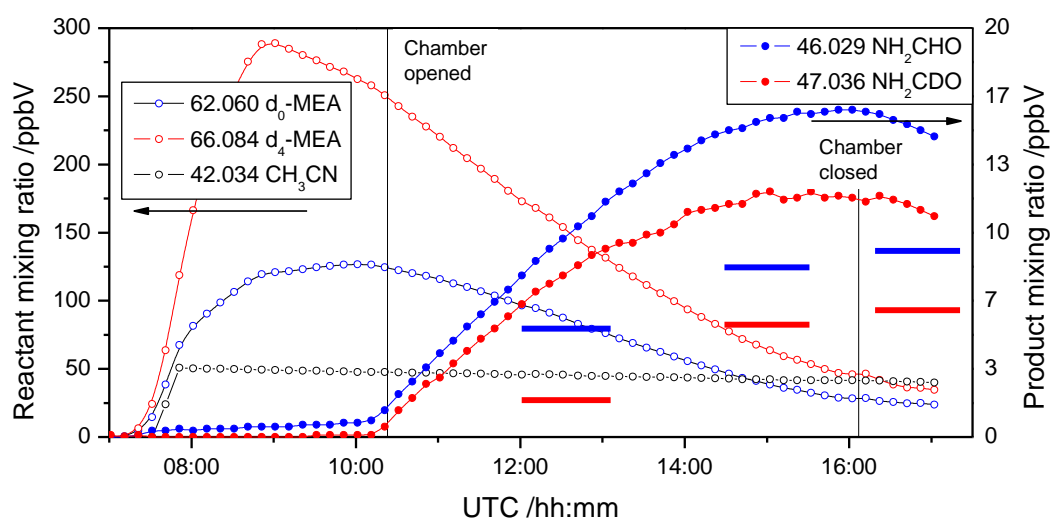
Figure 2.11. Time evolution of the m/z 62.060 (MEA), m/z 66.084 (MEA-d_4), m/z 42.034 (CH$_3$CN), m/z 46.029 (NH$_2$CHO) and m/z 47.036 (NH$_2$CDO) ion signals during the photo-oxidation experiment on May 19, 2009. The results from off-line analysis of Tenax TA adsorbent tubes are included for comparison; formamide (blue) and formamide-d_1 (red).

Figure 2.12 shows the time profiles of MEA as obtained by on-line PTR-TOF-MS and *in situ* FT-IR during the photo-oxidation experiment on May 15 illustrating the good agreement between the two methods. Filter samples were collected three times during the experiment and results from off-line analysis gave significantly higher average values: $<[MEA]>_1 = 3.05$ ppmV, $<[MEA]>_2 = 960$ ppbV, and $<[MEA]>_3 = 640$ ppbV. The figure also includes the FT-IR results for the NH_3 mixing ratio, which apparently increases throughout the experiment as long as the chamber canopy is open. The NH_3 mixing ratios were derived from the ro-vibrational lines of the v_2 (A_1) band employing line-strengths from the HITRAN data base.[23] It should be noted that the NH_3 formed does not stem from the gas phase photo-oxidation of MEA but rather from (un-quantifiable) surface reactions such as those suggested previously. It should also be noted that the amount of ammonia in the gas phase by far exceeds the total amounts of oxirane, ethylene glycol and glycolaldehyde together.
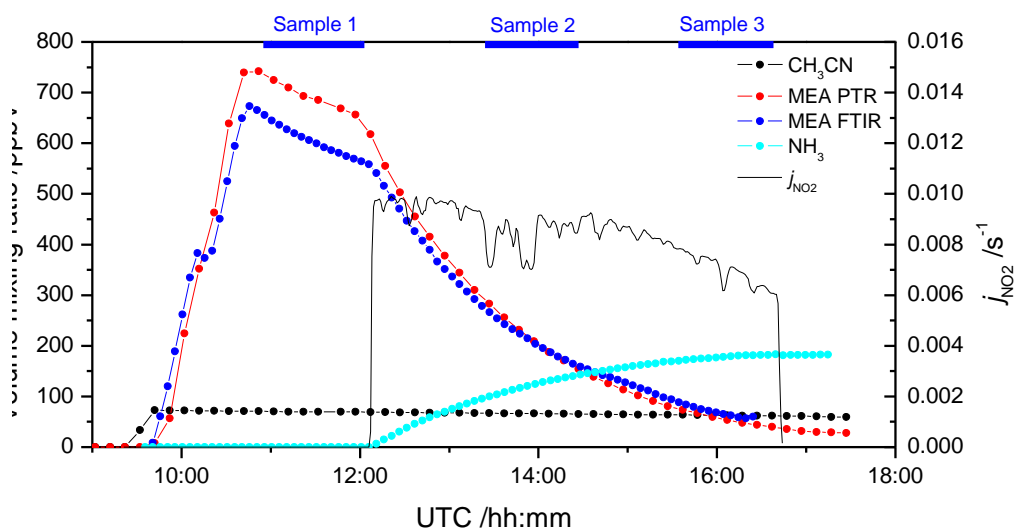
Figure 2.12. Photolysis frequency of NO_2 and time evolution of MEA (from PTR-TOF-MS and FT-IR), NH_3 (from FT-IR), and the tracer acetonitrile (from PTR-TOF-MS). Periods of sample collection are indicated on top of frame. Data from experiment on May 15, 2009.

Figure 2.13 compares the PTR-TOF-MS, FT-IR and Tenax TA adsorption tube results for the formamide volume mixing ratio during the experiment on May 15. The most characteristic infrared absorption band of formamide is overlapped by strong absorptions of water and concentration retrieval is difficult. In addition, there are no absolute infrared cross sections available for formamide (the vapour pressure at ambient temperatures is not known). The FT-IR results have therefore been scaled to the PTR-TOF-MS data. It can be seen that the formamide time-profiles from PTR-TOF-MS and FT-IR are in rough agreement. This also applies to the other experiments. The results from analyses of Tenax TA tubes apparently give systematically lower values than the PTR-TOF-MS instrument.
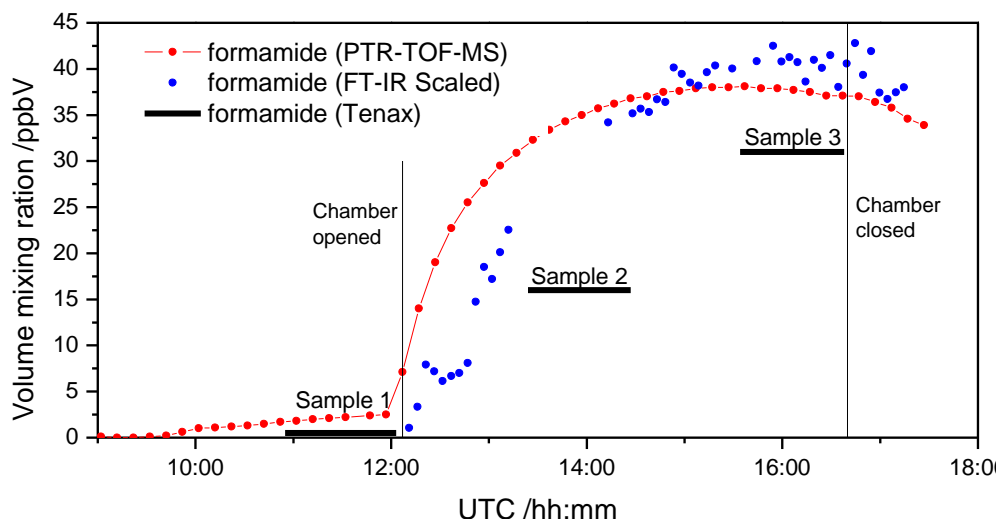
Figure 2.13. Time evolution of the photo-oxidation product formamide as measured by PTR-TOF-MS, FT-IR and Tenax. Data from experiment on May 15, 2009.

Two compounds of particular interest to the present study are the nitrosamine, $ONNHCH_2CH_2OH$ (2-(nitrosoamino) ethanol, CAS: 98033-27-3) and the nitramine, $O_2NNHCH_2CH_2OH$ (2-(nitroamino) ethanol, CAS: 74386-82-6), which may both be carcinogenic. The two compounds are not yet available as pure reference compounds and it is not clear if protonated ions are formed in unit yield in the PTR-TOF-MS instrument. Especially the protonated nitrosamine is anticipated to be unstable with the fragmentation pathways being unknown. The PTR-TOF-MS results must thus be interpreted with care.
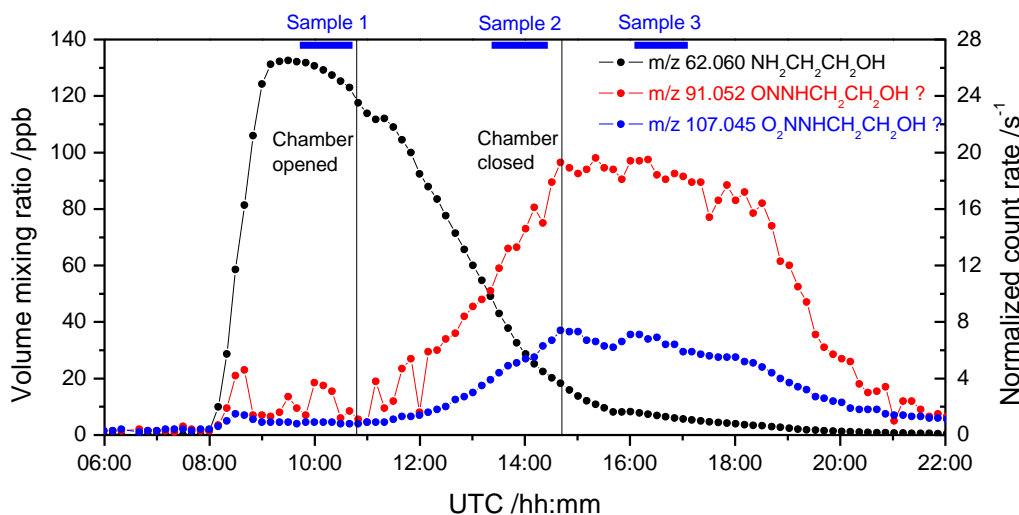
Figure 2.14. Time evolution of the ion signals at m/z 91.052 and m/z 107.045, corresponding to the exact masses of protonated $ONNHCH_2CH_2OH$ and $O_2NNHCH_2CH_2OH$, respectively. Periods of sample collection are indicated on top of frame. Data from experiment on May 10, 2009.

The PTR-TOF-MS signals at m/z 91.050 (the exact mass of the protonated nitrosamine) and at m/z 107.045 (the exact mass of the protonated nitramine) are displayed in Figure 2.14. The signal intensities are shown as normalized count rate (ncps) on the right-hand y-axis; a signal intensity of 28 ncps is equivalent to a volume mixing ratio of around 1 ppbV. Both ion signals are observed at <u>very</u> low intensities. We note that the m/z 91.050 peak could not be unambiguously
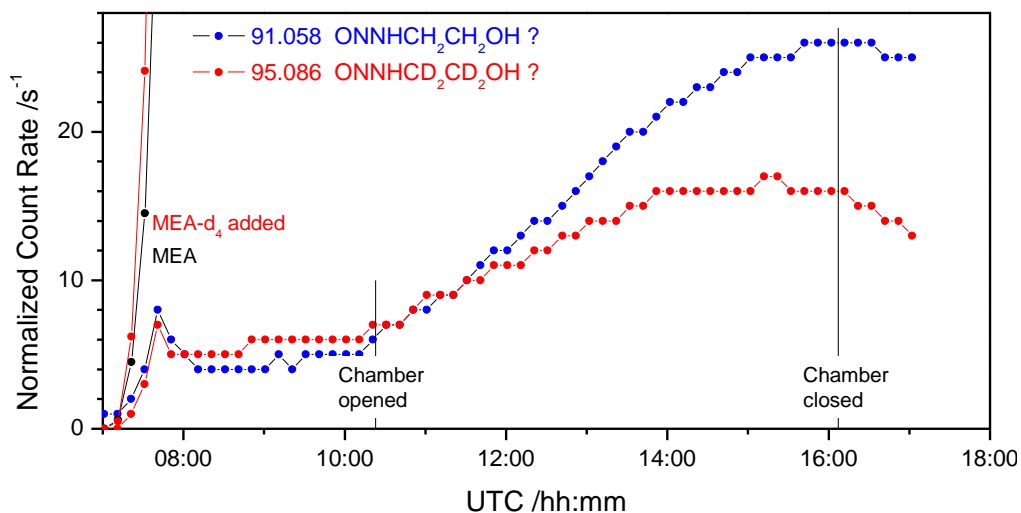
Figure 2.15. Time evolution of the ion signals at m/z 91.058 and m/z 95.086 corresponding to the exact masses of protonated ONNHCH$_2$CH$_2$OH and ONNHCD$_2$CD$_2$OH, respectively. Data from experiment on May 19, 2009.

resolved in the PTR-TOF-MS spectra. Furthermore, the time evolution of the m/z 91.050 signal is not as expected for a compound with a photolysis lifetime of only minutes ($j_{nitrosamine}$ ~0.5*j_{NO2}).[14]

Additional information is derived from the experiments with isotopically labelled MEA. In the experiment on May 19 a mixing ratio of around 1:2 between MEA and MEA-d$_4$ (see Figure 2.11) was obtained after adding MEA-d$_4$ to the chamber. The ion signals at m/z 91.050 and m/z 95.086, corresponding to the MEA and MEA-d$_4$ nitrosamines, respectively, are shown in Figure 2.15. First, the two ion signals have slightly different time evolutions, and, second, the m/z 91.050 signal exceeds the m/z 95.086 signal. This implies that the MEA nitrosamine, if formed at all, cannot be the only neutral parent compound forming the m/z 91.050 ion. Replacing all hydrogen atoms bonded to carbon by deuterium is not expected to <u>reduce</u> the amount of nitrosamine formed relative to the starting amount amine – rather the opposite is expected as a consequence of increasing the density of low-lying vibrational states in a reaction of the type RNH + NO → RNHNO‡. Under the (highly uncertain) assumption that protonated nitrosamine is formed in unit yield it is concluded that the amount of nitrosamine formed in the photo-oxidation of MEA is below 2 ‰ of the starting amine in the experiment on May 19. This conclusion is supported by the results from analyses of the Thermosorb/N adsorbent tubes, which showed no indications (<20 ng m^{-3} or <10 ppt) of nitrosamines being formed during any of the MEA photo-oxidation experiments (even if conducted with > 1 ppmV of MEA; see below). The origin of the m/z 91.058 and m/z 95.086 ion signals remain unknown.

The exact m/z's of protonated MEA and MEA-d$_4$ nitramines are m/z 107.045 and m/z 111.070, respectively. The two ion signals, observed in the May 19 experiments, are shown in Figure 2.16 and display a similar time evolution. The two ion signals were detected in a ~1:3 ratio, that is more O$_2$NNHCD$_2$CD$_2$OH than O$_2$NNHCH$_2$CH$_2$OH is formed relative to the amount of parent amine isotopologues, which is ~1:2, see Figure 2.11. The increased yield of nitramine

upon deuteration is in accord with the effect of an increase in density of low-lying vibrational states in an addition reaction. A search for the MEA nitramine in the various adsorbent tubes and filter samples collected during the May 19 experiment did not show the presence of nitramines in amounts above the detection limit (5 µg m^{-3} or around 1 ppbV).
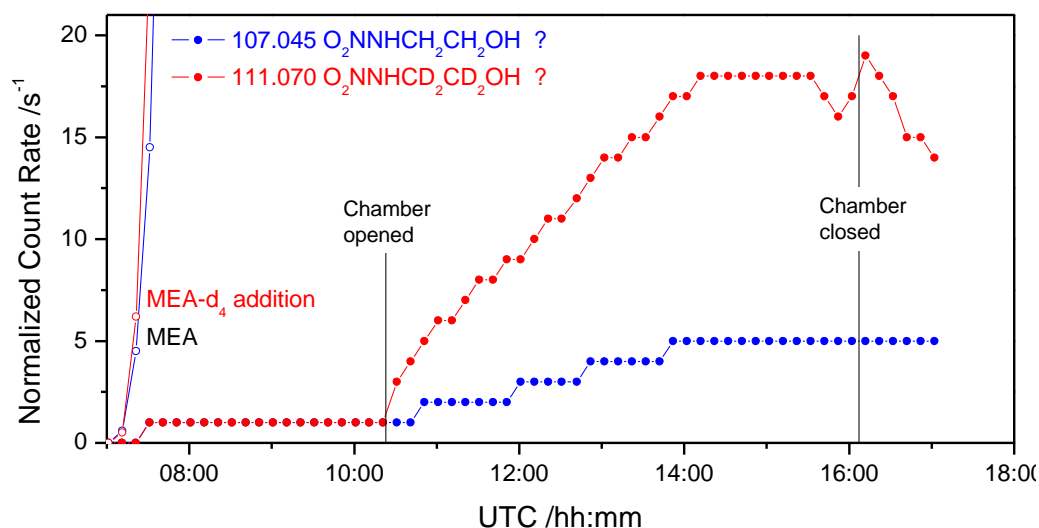
Figure 2.16. Time evolution of the ion signals at m/z 107.045 and m/z 111.070. Data from the experiment on May 19.

In the September 2009 experiments the starting concentrations of MEA were higher than in the May 2009 experiments. Figure 2.17 shows the time profile of MEA during the experiment on September 10. The figure also includes information on the NOx concentrations, j_{NO2}, and the periods of sample collection. The results from analyses of the Thermosorb/N adsorbent tubes, showed no indications (<20 ng m^{-3} or ~10 pptV) of the nitrosamine being present during the experiment. The results for the MEA nitramine were: Sample 1, <LoD; Samples 2-4, 15 ± 10 ppb. The high uncertainty in the amounts reported is linked to the lack of a pure reference compound (purification is going on at the time of writing). The identification, however, is unambiguous.
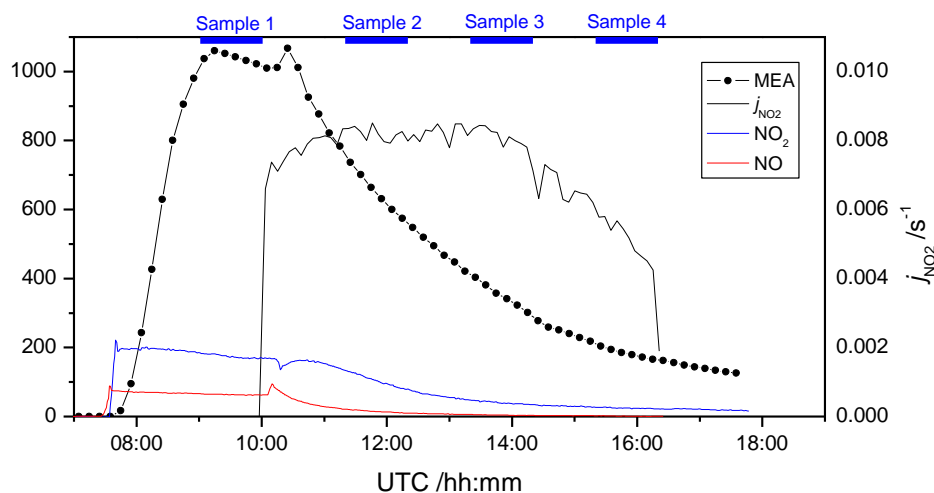
Figure 2.17. Photolysis frequency of NO$_2$, j_{NO2}, and the time evolution of MEA, NO and NO$_2$ during the photo-oxidation experiment on September 10. Periods of sample collection are indicated on top of frame.

2.4.2 Amine measurements

Comparisons of the amine concentrations obtained by PTR-TOF-MS, FT-IR and filter samples (compiled in section 9), show significant higher values for the filter samples than found by PTR-TOF-MS and FT-IR. One explanation for this discrepancy may be that MEA reacts with CO_2 under formation of 2-oxazolidone and water. The presence of 2-oxazolidone in the chamber could be confirmed by PTR-TOF-MS (m/z 88.039 with ion formula $C_3H_6O_2N$ in table 2.1) and is supported by Tenax analysis on the 11th of May with a decreasing concentration during the experiment. 2-oxazolidone may be produced in the heated MEA injection device and hence injected into the chamber, or it could be produced on the chamber walls with subsequent evaporation into the gas phase. Possible gas phase production is less likely but should not be excluded as a source without confirmation by real experiments. Unpublished laboratory test results indicate that the acidified filter surface of the off-line amine method will force the 2-oxazolidone formation equilibrium towards MEA and CO_2, which in turn imply that 2-oxazolidone collected on the filters will be measured as MEA. The FT-IR instrument will not observe 2-oxazolidone as MEA but as a completely different molecule, and the analysis results will be lower than the filter samples. One explanation for lower values in PTR-TOF-MS compared with off-line samples may be found in several differences between the filter inlet lines and the PTR- TOF-MS inlet line, where a possible artifact (m/z 60.044 with ion formula C_2H_6NO) may be explained by a MEA rearrangement on heated surfaces. Within the frame of this project it is not feasible to draw a robust conclusion of the amine measurement discrepancies. Due to the significant differences in the measurement results, the model calculations should be performed with two different scenarios; one with data provided from PTR-TOF-MS/FT-IR analysis and one with data provided from off-line measurements. It is also recommended to perform separate comparison experiments for the PTR-TOF-MS, FT-IR and off-line methods. In addition, it is recommended to take a closer look at the surface chemistry both with theoretical considerations and experiments.

2.4.3 Summary of experiment interpretation

In every smog-chamber there are a number of "chamber artefacts" which, if not identified as artefacts, can lead to erroneous conclusions. A series of chamber artefacts and a number of specific reaction products originating from heterogeneous wall and/or particle surface reactions of MEA have been identified. The use of stable MEA isotopologues has been invaluable in isolating "MEA-chemistry" from chamber artefacts.

Of the around 30 ion signals, registered by PTR-TOF-MS and with intensities above 1 % of the initial MEA ion signal, only 4 corresponded exactly to those of the theoretically predicted products. Nine of the observed product ion signals stem from N-containing C_3 and C_4 compounds. Experiments with stable isotopologues of MEA showed that these compounds originate from surface-assisted condensation reactions between MEA various aldehydes, ketones, carboxylic acids and imines.

The integration of *in situ*, on-line and off-line techniques made it possible to identify or tentatively identify nearly every ion signal ($I_m > 1\%$ of $\Delta I_{62.060}$ (MEA)) registered by PTR-TOF-MS and to resolve ambiguities related to structural isomerism.

The major products from gas phase photo-oxidation of MEA identified by various analytical techniques are formamide, $CHONH_2$, and formaldehyde, CH_2O. We have found experimental evidence that amino acetaldehyde, NH_2CH_2CHO, and/or 2-imino ethanol, $HN=CHCH_2OH$, and 2-oxo acetamide, $NH_2C(O)CHO$ are formed as minor products. The nitramine 2-(nitroamino) ethanol, $O_2NNHCH_2CH_2OH$, has been unambiguously identified as a minor product in the MEA photo-oxidation.

2.5 Effect of elevated water vapour concentrations in the EUPHORE chamber

It was originally the intention to study MEA photo-oxidation of under humid and high-NOx conditions mimicking the situation near an emission source. It turned out, however, that the loss of MEA from the gas phase to chamber walls and particles was so fast under humid conditions that it was not possible to observe any photo-oxidation. Figure 2.18 shows the time profile of MEA in an experiment with around 20 % relative humidity. Essentially, the MEA loss can be described by a single exponential decay with a lifetime of 1 hour.
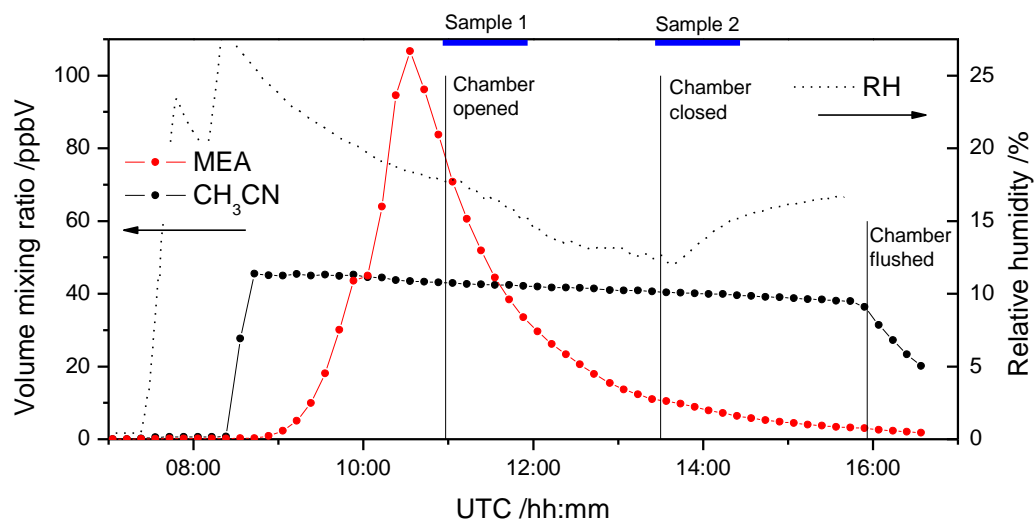
Figure 2.18. Effect of increased relative humidity in a EUPHORE chamber experiment with MEA. Data from experiment on May 12, 2009.

In the following it is discussed which medium has the higher potential for liquid phase uptake of MEA: the chamber walls or the aerosol formed in the photo-oxidation of MEA. The consideration is done for the assumption that an equilibrium between the gas phase and the liquid phase was established in the chamber. The gas phase/liquid phase equilibrium partitioning is described by the Henry's Law coefficient. The Henry Law coefficient of MEA is 6.2×10^6 M atm^{-1}.[35] Water vapour adsorbs to Teflon walls following a BET adsorption expression. According to the empiric parameterization by Svensson *et al.*,[36] the amount of

adsorbed water on the chamber wall of EUPHORE at 18% relative humidity is calculated to be 2.1 mg m^{-2} (3-6 mono layers for a 2-3 Å^2 site area) corresponding to L_{wall} = 2.4×10^{-12} dm^3 cm^{-3} (chamber volume: 177 m^3, chamber surface area: 200 m^2). The transfer coefficient for the exchange of MEA between chamber air and foil surface is limited by the laminar boundary layer and is calculated to be 9.4×10^{12} s^{-1}. After MEA was added to the chamber a concentration maximum of 107 ppbV (measured by PTR-TOF-MS at 10:33 UTC) was reached before MEA concentrations fell steeply off. Based on Henry's Law, the corresponding aqueous phase concentration of MEA in the water film on the Teflon foil was 9.4×10^{11} molec cm^{-3} (of air). Particles formed after the chamber was opened, but numbers were two orders of magnitude lower than in the dry experiments. Using the empirical polynomials by Tang and Munkelwitz for calculating the water content on ammonium sulphate particles,[37] the total liquid amount of adsorbed water on chamber aerosols is L_{aer} = 2.1×10^{-13} dm^3 cm^{-3} at the time of opening the chamber canopy. For droplets, gas phase and interfacial mass transfer limitation have to be taken into account. The geometric mean diameter of the initial aerosol was 58 nm. From this and the molecular parameters of MEA, the mass transfer coefficient k_{mt},[38] is calculated to be 7.5×10^7 s^{-1}. This corresponds to a MEA uptake rate of 1.0×10^{-10} s^{-1} to the wet aerosol. It is concluded that the uptake of MEA to the wetted chamber wall is about 6 orders of magnitude faster than its corresponding uptake to the wet chamber aerosol.

The lifetime of MEA towards the gas phase reaction with OH in the experiments is typically 8 hours (assuming [OH]=1x10^6 molec cm^{-3} and k_{OH}=3.4×10^{-11} cm^3 s^{-1}). The decay of MEA in the humid experiment occurred at a rate which was several times faster than in the dry experiments. From the discussion above it is concluded that uptake of MEA to the water film of the chamber wall was the main loss process. The lifetime of MEA towards uptake to the liquid phase of the walls is estimated to be 1 hr. Thus uptake of MEA to wetted surfaces is 8 times faster than chemical degradation in the humid experiment and the wet wall loss rate is about 1×10^{-4} s^{-1}, *i.e.* 3-5 times faster than the dry wall loss rate

3 Gas phase photochemistry mechanism

The photo-oxidation of MEA is initiated in H-abstraction reactions by OH radicals:

$$NH_2CH_2CH_2OH + OH \xrightarrow{k_1} NH_2CH_2CH_2\dot{O} + H_2O \qquad (1)$$

$$\xrightarrow{k_2} NH_2CH_2\dot{C}HOH + H_2O \qquad (2)$$

$$\xrightarrow{k_3} NH_2\dot{C}HCH_2OH + H_2O \qquad (3)$$

$$\xrightarrow{k_4} \dot{N}HCH_2CH_2OH + H_2O \qquad (4)$$
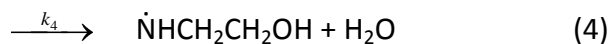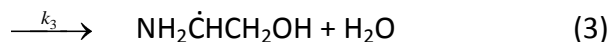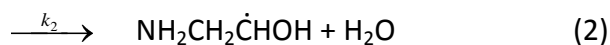
There is no experimental value for $k_{tot} = k_1 + k_2 + k_3 + k_4$, and there are no experimental values for the branching ratio in the N-H : C-H abstraction reaction by OH radicals in primary amines. An estimated value of $k_{tot} = 3.1 \times 10^{-11}$ cm^3 molecule^{-1} s^{-1}, may be obtained from $k_{tot} \approx k_{OH+CH_3CH_2OH} + k_{OH+CH_3CH_2NH_2}$, where $k_{OH+CH_3CH_2OH} = 3.2 \times 10^{-12}$,[39] and $k_{OH+CH_3CH_2NH_2} = 2.8 \times 10^{-11}$ cm^3 molecule^{-1} s^{-1}.[5, 40] A critical review of results from numerous studies of the CH$_3$CH$_2$OH + OH reaction has led to the conclusion that H-abstraction from the CH$_2$-group accounts for 90 %, while H-abstraction from the methyl- and hydroxyl groups each accounts for 5 % of the total CH$_3$CH$_2$OH reactivity towards OH. Consequently, a first approximation to k_1 through k_4 will be: $k_1 \approx 1.6 \times 10^{-13}$, $k_2 \approx 2.9 \times 10^{-12}$, and $k_3 + k_4 \approx 2.8 \times 10^{-11}$ cm^3 molecule^{-1} s^{-1}.

The absolute value of k_{tot} is not pertinent to the following discussion of the relative importance of the four reaction routes. The total loss of MEA from the gas phase depends upon k_{tot} *times* [OH]$_t$; the branching ratios only depend upon the relative values of k_1 - k_4 and are thus independent of [OH]$_t$ which, for the present purpose, may by adjusted to scale the model to the observations.

3.1 $NH_2CH_2CH_2OH \xrightarrow{Ox} NH_2CH_2CHO.$

From the above route (1) is expected to account for less than 1 % of the MEA reactivity towards OH radicals; the products of this route are essentially the same as those resulting from H-abstraction from C$_1$ although internal 1,4-Hydrogen shift may constitute a very minor route leading to the same amino radical as formed in route (4):

$$NH_2CH_2CH_2\dot{O} + O_2 \longrightarrow NH_2CH_2CHO + HO_2 \qquad (5)$$

$$\xrightarrow{1,4} \dot{N}HCH_2CH_2OH \qquad (6)$$
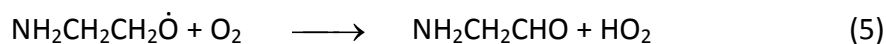
For all practical purposes routes (1) and (2) will therefore result in the same primary product, amino acetaldehyde:

$$NH_2CH_2\dot{C}HOH + O_2 \longrightarrow NH_2CH_2CHO + HO_2 \qquad (7)$$
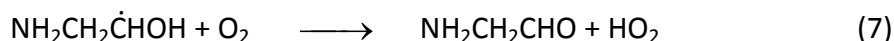
There are indications that a small amount of amino acetaldehyde is being formed in the photo-oxidation of MEA. The PTR-TOF-MS data suggest a peak mixing ratio of around 1.5 ppbV in the experiment on May 10, see Figures 2.5-2.7, but quantification is questionable (see below). Off-line analysis of DNPH cartridges suggest a maximum value of 0.04 ppbV in this experiment. The small amounts of amino acetaldehyde observed as a photo-oxidation product is interpreted in terms of $k_2 \ll k_{tot}$. It is, however, not clear how quantitative the two methods

are since the pure reference compound is not available for testing. Amino acetaldehyde is an evasive compound which polymerises as soon as formed in the liquid. Like other aldehydes, it is also expected to undergo condensation reactions with amines on surfaces. The small amounts of amino acetaldehyde observed could alternatively be interpreted in terms of the compound reacting on the surfaces of the chamber, on the surfaces in the DNPH cartridges before being derivatized or in the tubing connecting the chamber to the PTR-TOF-MS and the air sampling filters and cartridges. Accurate quantification of amino acetaldehyde by PTR-TOF-MS may be complicated by the presence of isomeric species (*e.g.* acetamide or 2-imino ethanol). In addition, protonated amino acetaldehyde may be unstable in the PTR-TOF-MS reaction chamber and decompose to form protonated ammonia and/or protonated glycolaldehyde, two ions which were detected in substantial abundances (same ion chemistry mechanism as described later for its structural isomer 2-imino ethanol).

According to the PTR-TOF-MS data ca. 20 ppbV NH_2CHO and ca. 1.5 ppbV $NH_2C(O)CHO$ were formed during 2 hours of photo-oxidation of around 100 ppbV MEA in the May 10 experiment (see Figure 2.5). It should be noted that 2-oxo acetamide, $NH_2C(O)CHO$, was not observed by the off-line methods and that its identification in the PTR-TOF mass spectra has to be considered as being tentative. The experiment was a high-NOx experiment with average mixing ratios of NO and NO_2 around 300 and 50 ppbV, respectively. A simple analysis suggests that a value of $k_3 \approx 2.9 \times 10^{-11}$ cm^3 molecule^{-1} s^{-1}, and an average [OH] = 10^6 molecules cm^{-3} will reproduce the observed formaldehyde time profile and k_2/k_{tot} = 0.08 will result in the formation of around 1.5 ppbV NH_2CH_2CHO from the MEA reaction with OH. Even with $k_{OH+NH_2CH_2CHO} = 1.0 \times 10^{-10}$ cm^3 molecule^{-1} s^{-1}, which is 10 times the value of the rate constant for the reaction of CH_3CHO with OH radicals,[39] less than half of the formed NH_2CH_2CHO will react with OH in the same time slot. The two additional routes leading from amino acetaldehyde to formamide (photolysis and H_{ald}-abstraction) will also reduce the 2-oxo acetamide yield. These routes cannot, however, be quantified on the basis of the present data.

The results from off-line analysis of DNPH cartridges collected on May 10 suggest that only 0.04 ppbV NH_2CH_2CHO is formed in the experiment. This result places k_2/k_{tot} <0.01. It is thus unlikely that the observed formation of as much as 1.5 ppbV 2-oxo acetamide, $NH_2C(O)CHO$, in this experiment originates exclusively from photo-oxidation of NH_2CH_2CHO, which, in turn, was formed in the photo-oxidation of MEA. 2-Oxo acetamide may also be formed in the photo-oxidation of acetamide, which was detected in the Tenax TA adsorbtion tubes:

$$NH_2C(O)CH_3 + OH \xrightarrow{k_8} NH_2C(O)\dot{C}H_2 + H_2O \qquad (8)$$

$$NH_2C(O)\dot{C}H_2 + O_2 \longrightarrow NH_2C(O)CH_2O\dot{O} \qquad (9)$$

$$NH_2C(O)CH_2O\dot{O} + NO \longrightarrow NH_2C(O)CH_2\dot{O} + NO_2 \qquad (10)$$

$$NH_2C(O)CH_2\dot{O} + O_2 \longrightarrow NH_2C(O)CHO + HO_2 \qquad (11)$$
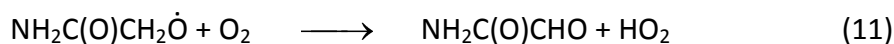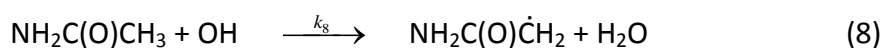
There is no rate constant available for the acetamide reaction with OH. Assuming that the m/z 60.044 ion signal detected before opening of the chamber canopy is

entirely due to acetamide and taking k_8 = 1.0 × 10^{-11} cm^3 molecule^{-1} s^{-1} (a conservative upper limit estimate) will give around 0.7 ppb 2-oxo acetamide, which is only half of what is observed.

One extreme scenario is that all amino acetaldehyde formed in the photo-oxidation of MEA reacts with amines (MEA) on surfaces. In this case, the resulting imine, $NH_2CH_2CH=NCH_2CH_2OH$, should reach ppb concentration even if it reacts fast with OH and/or O_3. Although it is unclear if the PTR-TOF-MS quantitatively detects imines, see later, the obtained results however suggests that the $NH_2CH_2CH=NCH_2CH_2OH$ mixing ratio is closer to pptV-levels than to ppbV-levels. Another extreme scenario is that all amino acetaldehyde formed polymerizes on chamber walls, particles and in the tubing connecting the chamber with the instrumentation and filter sampling units. In this case the amount of 2-oxo acetamide, a secondary photo-oxidation product, is the only lead to the branching ratio.

The assumption that the *additional* m/z 60.044 ion signal stem 100 % from amino acetaldehyde leads to a branching ratio of k_2/k_{tot} = 0.08. Taking the off-line analysis result for the maximum volume mixing ratio of amino acetaldehyde to be 0.04 leads to k_2/k_{tot} < 0.01.

The May 11 experiment was a high-NOx experiment with NO and NO$_2$ mixing ratios around 700 and 350 ppbV, respectively. This extreme NOx mixing ratio mimics the situation close to the point of emission from a CCS-plant. The PTR-TOF-MS data suggest that in this experiment ca. 7 ppbV NH_2CHO and ca. 0.6 ppbV $NH_2C(O)CHO$ were formed during 4 hours of photo-oxidation of around 80 ppbV MEA. The high NOx-level suppresses OH and the observed amount and time profile of formamide requires a concentration of 4.5×10^5 molecules cm^{-3} for k_3 = 2.8 × 10^{-11} cm^3 molecule^{-1} s^{-1}. No additional (intermediate) m/z 60.044 ion signal was observed by PTR-TOF-MS in this experiment, and the results from off-line analysis of DNPH cartridges for amino acetaldehyde give a maximum of 0.03 ppbV. Again, it is not possible to reproduce a mixing ratio of 0.6 ppbV for 2-oxo acetamide unless arising from photo-oxidation of acetamide or from 1.5 ppbV of amino acetaldehyde which is not observed. Assuming a maximum amino acetaldehyde mixing ratio of 0.03 ppbV places k_2/k_{tot} to <0.01. Taking the 0.5 ppbV as a threshold for observing an additional m/z 60.044 ion signal from amino acetaldehyde places an upper limit of 0.05 for k_2/k_{tot}.

On May 14, the starting volume mixing ratio of MEA was higher than on May 11, amounting to approximately 700 ppbV. The NO and NO$_2$ mixing ratios were around 1300 and 20 ppbV, respectively, at start, and around 700 and 350 ppbV, respectively, towards the end of the experiment. In this photo-oxidation experiment around 50 ppbV of formamide and around 2.5 ppbV of 2-oxo acetamide were formed during 4 ½ hours. The amount and time profile of the formamide formed requires a concentration of 4.5×10^5 molecules cm^{-3} for k_3 ≈ 2.8×10^{-11} cm^3 molecule^{-1} s^{-1}. Neglecting potential fragmentative loss of protonated amino acetaldehyde or interference from isomers, the observed increase in the PTR-TOF-MS m/z 60.044 ion signal is estimated to be equivalent to the formation of 2.5-3 ppbV of amino acetaldehyde. This can be reproduced

using $k_2/k_{tot} \approx 0.06$, but to reproduce a mixing ratio of around 2.5 ppbV for 2-oxo acetamide $k_{OH+NH_2CH_2CHO}$ has to be near the collision limit. Again, the observed formation of 2-oxo acetamide requires an additional source. The results from off-line analysis of DNPH cartridges give a maximum amino acetaldehyde mixing ratio of only 0.04 ppbV, which places k_2/k_{tot} <0.01.

The experiment on May 15 is an extremely low-NOx experiment with NO around 5 and NO_2 around 10 ppbV, and a relative humidity around 0.5 %. The walls are thus activated with respect to H_2O and MEA wall loss is a dominant process. This experiment mimics the situation in a Norwegian rural environment. During the 3 ½ h experiment the MEA mixing ratio dropped from around 600 to 35 ppbV. At the same time, formamide increased by 30 ppbV and 2-oxo acetamide by 2.5 ppbV. Figure 2.7 shows that the m/z 60.044 ion signal increased by around 4 ppbV shortly after opening of the canopy. These observations can be reproduced with $k_2/k_{tot} \approx 0.12$ and $k_{OH+NH_2CH_2CHO} = 5.0 \times 10^{-11}$ cm^3 molecule^{-1} s^{-1}. The results from off-line analysis of DNPH cartridges give a maximum amino acetaldehyde mixing ratio of 0.03 ppbV, which places k_2/k_{tot} to <0.01.

The atmospheric fate of NH_2CH_2CHO appears to be dominated by hydrogen abstraction from the CH_2-group although photolysis and hydrogen abstraction from the aldehyde group cannot be ruled out. We did, however, not observe any evidence for the formation of the PAN-like peroxy nitrate, $NH_2CH_2COONO_2$, which is normally expected following hydrogen abstraction from an aldehyde group. At this stage it is, however, not clear if analytical problems prevented the detection of PAN-type compounds.

Scheme 3.1 summarises the photo-oxidation routes of MEA following initial hydrogen abstraction from the CH_2OH group. Assuming that the increase in the m/z 60.044 PTR-TOF-MS ion signal is entirely due to amino acetaldehyde an average branching ratio of $k_2/k_{tot} = 0.08 \pm 0.03$ can be derived. Based upon the off-line analyses of DNPH cartridges a branching ratio k_2/k_{tot} <0.01 is found. In neither case is it possible to explain the observed increase in the m/z 74.024 ion signal (2-oxo acetamide) by further reaction of amino acetaldehyde.
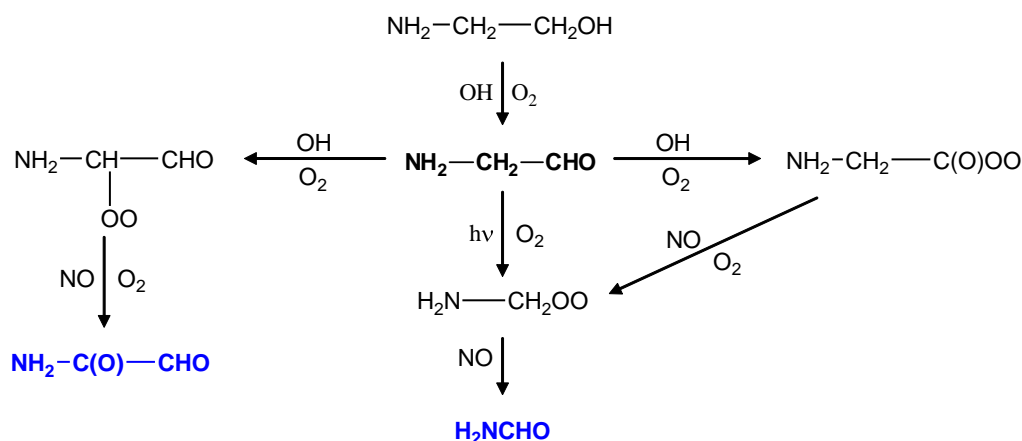
Scheme 3.1. Atmospheric photo-oxidation of MEA following hydrogen abstraction from the -CH$_2$OH group.

3.2 NH$_2$CH$_2$CH$_2$OH $\xrightarrow{Ox}$ NH$_2$CH(O)CH$_2$OH radical.

The H-abstraction reaction at C$_2$ will, under atmospheric conditions, be followed by addition of O$_2$ to form a dioxy radical. The main fate of this radical, in turn, will be reaction with NO to form an oxy radical:

$$NH_2\dot{C}HCH_2OH + O_2 \longrightarrow NH_2CH(O\dot{O})CH_2OH \qquad (12)$$

$$NH_2CH(O\dot{O})CH_2OH + NO \longrightarrow NH_2CH(\dot{O})CH_2OH + NO_2 \qquad (13)$$
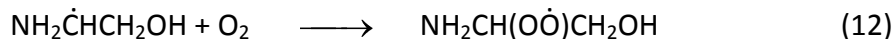
In general, the fate of oxy radials includes isomerisation, H$_\alpha$-abstraction and dissociation. In the present case, the isomerisation reaction (1,4-H shift) is too slow to be of importance, and only the two other routes are relevant under atmospheric conditions:

$$NH_2CH(\dot{O})CH_2OH \xrightarrow{\Delta} NH_2CHO + CH_2OH \qquad (14)$$

$$NH_2CH(\dot{O})CH_2OH + O_2 \longrightarrow NH_2C(O)CH_2OH + HO_2 \qquad (15)$$
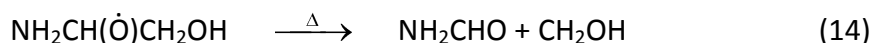
Reaction (14) is exothermic by ca. -35 kJ mol^{-1},[1] and the estimated unimolecular rate constant, k_{10}, will therefore be huge, around 10^{10} s^{-1},[2] which is 5 orders of magnitude faster than k_{11}*[O$_2$] $\approx 10^5$ s^{-1}. Analysis of the Tenax TA tubes did not show any trace of hydoxyacetamide, NH$_2$C(O)CH$_2$OH, and the PTR-TOF-MS showed no discernible increase in the m/z 76.054 ion signal, corresponding to C$_2$H$_6$NO$_2^+$, protonated hydroxyacetamide.

The CH$_2$OH radical formed in (14) will undergo fast H-abstraction by O$_2$ resulting in formaldehyde:

$$\dot{C}H_2OH + O_2 \longrightarrow CH_2O + HO_2 \qquad (16)$$
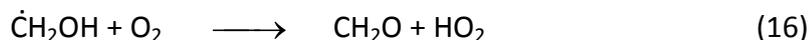
It is concluded that H-abstraction from the C$_2$-position will give NH$_2$CHO + CH$_2$O as products in a yield close to 100 %.

Deuterium substitution of hydrogen bonded to the carbon atoms slows down the rate of reaction with OH radicals. Figure 2.10 illustrates that less CDONH$_2$ than CHONH$_2$ is formed in the chamber in spite of there being more MEA-d$_4$ than MEA in the gas phase in the experiment on May 19. The formation of CHONH$_2$ and CDONH$_2$, respectively, was modelled assuming an average OH concentration of 4.5×10^5 molecules cm^{-3} throughout the experiment. Although the assumption of a constant OH field is clearly inadequate, an approximate kinetic isotope effect $k_{H_2NCH_2CH_2OH+OH}$ / $k_{H_2NCD_2CF_2OH+OH}$ of around 2.5 may be extracted from the data, Figure 3.1. The major problem in analysing the data is linked to the different aerosol and wall losses of MEA and MEA-d$_4$. However, this ambiguity has little influence on the derived kinetic isotope effect.
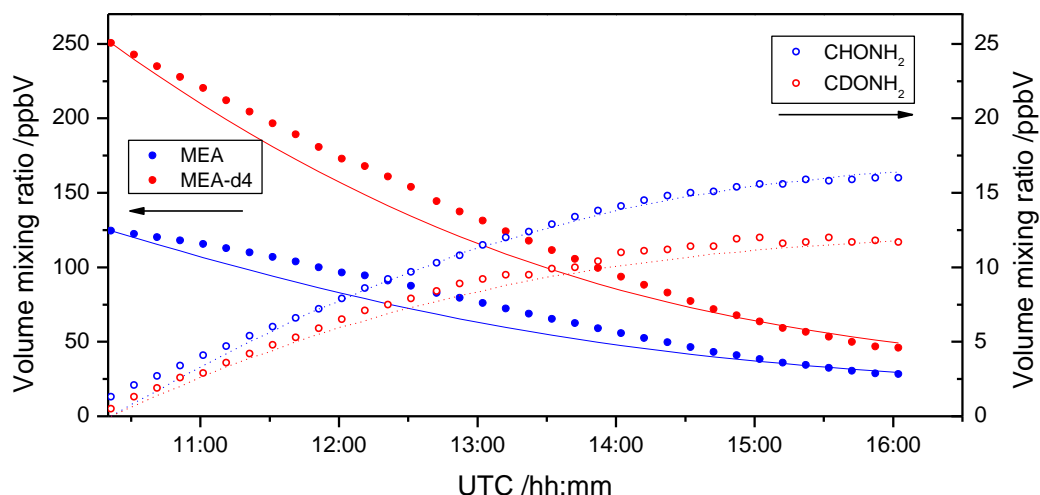
Figure 3.1. Plot of Observed and calculated volume mixing ratios of MEA, MEA-d$_4$, CHONH$_2$ and CDONH$_2$ during the experiment on May 19.

Hydrogen abstraction from the –CH$_2$– group constitutes the major route in the atmospheric photo-oxidation of MEA. It is estimated, see later, that >80 % of the OH initiated photo-oxidation will result in the formation of formamide and formaldehyde according to Scheme 3.2.
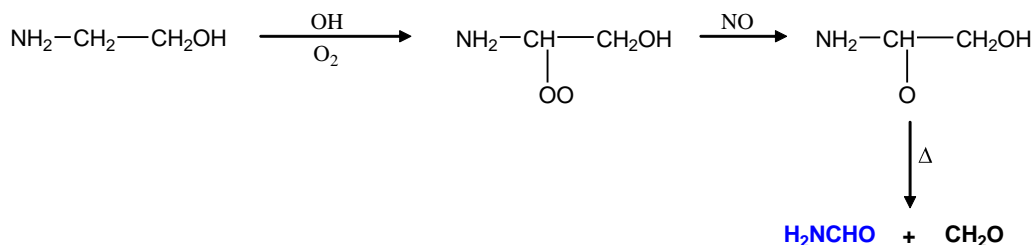
Scheme 3.2. Atmospheric photo-oxidation of MEA following hydrogen abstraction from the -CH$_2$- group.

3.3   NH$_2$CH$_2$CH$_2$OH $\xrightarrow{Ox}$ NHCH$_2$CH$_2$OH radical.

The amount of O$_2$NNHCH$_2$CH$_2$OH formed in the photo-oxidation experiments suggests that $k_4 < k_3$. In fact, the PTR-TOF-MS results suggest that less than 0.3 ppbV O$_2$NNHCH$_2$CH$_2$OH was formed in the May 10 experiment. *It is stressed that this compound is not yet available as a pure reference, and that it is not clear if protonated ions of O$_2$NNHCH$_2$CH$_2$OH are formed in unit yield in the PTR-TOF-MS instrument. The volume mixing ratios presented for the nitramine have thus to be considered as being tentatitve only.* The results from samples collected on adsorbents during this experiment show no indications of O$_2$NNHCH$_2$CH$_2$OH (LoD <5 μg m^{-3}/1 ppbV).

The reactions leading to the formation of the nitrosamine and nitramine are:

$$NH_2CH_2CH_2OH + OH \longrightarrow \dot{N}HCH_2CH_2OH + H_2O \qquad (4)$$

$$\dot{N}HCH_2CH_2OH + NO \longrightarrow ONNHCH_2CH_2OH \qquad (17)$$

$$ONNHC(O)CH_2OH \xrightarrow{h\nu} \dot{N}HCH_2CH_2OH + NO \qquad (18)$$

$$\dot{N}HCH_2CH_2OH + O_2 \longrightarrow NH{=}CHCH_2OH + HO_2 \qquad (19)$$

$$\dot{N}HCH_2CH_2OH + NO_2 \longrightarrow NH{=}CHCH_2OH + HONO \qquad (20)$$

$$\longrightarrow O_2NNHCH_2CH_2OH \qquad (21)$$
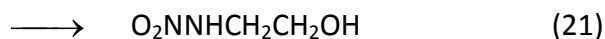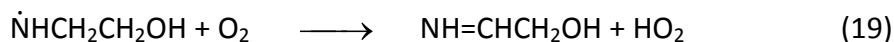
An estimate of k_4 may be obtained by assuming the reaction rate constants $k_{tot} = 3.1 \times 10^{-11}$ cm^3 molecule^{-1} s^{-1}, and $k_{17} - k_{21}$ to have the same values as in the corresponding reactions of dimethylamine: $k_{17} = 8.5 \times 10^{-14}$, $k_{19} = 1.2 \times 10^{-19}$, $k_{120} = 3.2 \times 10^{-13}$, and $k_{21} = 7.0 \times 10^{-14}$ cm^3 molecule^{-1} s^{-1}. [12, 41] The photolysis rate constant $j_{14} = 0.53 \times j_{NO_2}$ is taken from the work of Tuazon et al,[14] which corresponds to an average rate of $\approx 4 \times 10^{-3}$ s^{-1} during the experiment on May 10. Assuming that there are no other loss and formation processes than those given above the differential rate laws to be solved are:

$$\frac{d[MEA]}{dt} = -k_{tot} \cdot [MEA] \cdot [OH]$$

$$\frac{d[A]}{dt} = k_4 \cdot [MEA] \cdot [OH] - k_{17} \cdot [A] \cdot [NO] - k_{19} \cdot [A] \cdot [O_2]$$
$$- (k_{20} + k_{21}) \cdot [A] \cdot [NO_2] + j_{18} \cdot [ANO]$$

$$\frac{d[ANO]}{dt} = k_{17} \cdot [A] \cdot [NO] - j_{18} \cdot [ANO]$$

$$\frac{d[IM]}{dt} = (k_{19} \cdot [O_2] + k_{20} \cdot [NO_2]) \cdot [A]$$

$$\frac{d[ANO_2]}{dt} = k_{21} \cdot [A] \cdot [NO_2]$$

where: MEA = NH$_2$CH$_2$CH$_2$O; A = $\dot{N}$HCH$_2$CH$_2$OH; ANO = ONNHCH$_2$CH$_2$OH; IM = NH=CHCH$_2$OH, and ANO$_2$ = O$_2$NNHCH$_2$CH$_2$OH.

The above set of equations may be solved in the steady-state approximation giving:

$$[ANO]_{ss} = \frac{k_{17} \cdot [A] \cdot [NO]}{j_{18}}$$

$$[A]_{ss} = \frac{k_4 \cdot [MEA] \cdot [OH]}{k_{19} \cdot [O_2] + (k_{20} + k_{21}) \cdot [NO_2]}$$

from which the imine (IM) and nitramine (ANO$_2$) concentrations may be derived by numerical integration.

In the May 10 experiment around 0.3 ppbV O$_2$NNHCH$_2$CH$_2$OH and 20 ppbV NH$_2$CHO were formed in the photo-oxidation of MEA during 2 hours. This corresponds to a molar nitramine yield of $\approx$ 1.3 %. The experiment was a high-NOx experiment with average mixing ratios of NO and NO$_2$ around 300 and 50

ppbV, respectively. To get the amounts mentioned requires an average [OH] of 1×10^6 molecules cm^{-3} and $k_4 \approx 0.12 \times k_{tot}$. The chemistry model predicts that the amount of nitrosamine in the chamber will always be below 50 pptV and that the amount of NH=CHCH$_2$OH formed could ultimately reach around 2 ppbV in this experiment.

In the May 11 experiment ca. 0.14 ppbV O$_2$NNHCH$_2$CH$_2$OH and ca. 7 ppbV NH$_2$CHO were formed during 4 hours of photo-oxidation of MEA under extremely high NOx conditions, and the molar nitramine yield is $\approx$ 1.5 %. To get the amounts mentioned requires an average [OH] of 4.5×10^5 molecules cm^{-3} and $k_4/k_{tot} \approx 0.07$. The chemistry model predicts that the amount of nitrosamine in the chamber will always be below 10 pptV and that the amount of imine formed may reach around 0.1 ppbV in this experiment.

On May 14, which is also an extreme NOx-experiment, the MEA nitramine is formed in around 0.5 ppbV and formamide in around 50 ppbV (according to PTR-TOF-MS). This correspond to a molar nitramine yield of $\approx$ 0.6 %. To reproduce a mixing ratio of around 0.5 ppbV for O$_2$NNHCH$_2$CH$_2$OH requires $k_4/k_{tot} \approx 0.07$. The maximum mixing ratio of imine formed is predicted to be around 1.7 ppbV.

The May 15 experiment was an extremely low-NOx experiment with average NO and NO$_2$ mixing ratios of 5 and 10 ppbV, respectively. Around 0.15 ppbV O$_2$NNHCH$_2$CH$_2$OH and 40 ppbV NH$_2$CHO were formed in the photo-oxidation of around 400 ppbV MEA during 4 hours. The molar nitramine yield is only $\approx$ 0.3 %. To get the amounts mentioned requires an average [OH] of 4×10^5 molecules cm^{-3} and $k_4/k_{tot}.$ = 0.05. The maximum mixing ratio of imine formed is predicted to be around 2.2 ppbV.

The main conclusion to be drawn from the analyses of the nitramine formation is that as much as 10 % of the initial H-abstraction in MEA by OH radicals takes place at the amino group. It is stressed that the branching ratio k_4/k_{tot} has been derived from the amount of O$_2$NNHCH$_2$CH$_2$OH determined by PTR-TOF-MS in the experiments, and the assumption that the other relevant reaction and photolysis rate constants have the same values as in the corresponding reactions of dimethylamine.[12, 41]

Scheme 3.2. summarises the atmospheric photo-oxidation of MEA following hydrogen abstraction from the NH$_2$-group. Although actually not detected in the
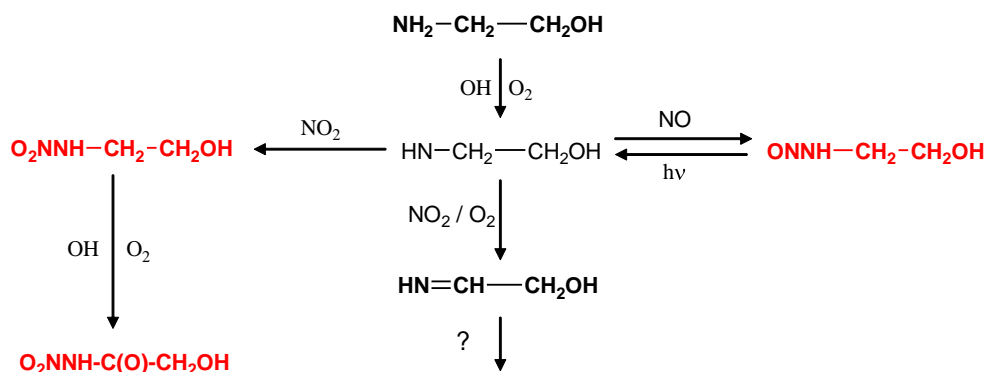
Scheme 3.2. Atmospheric photo-oxidation of MEA following hydrogen abstraction from the NH$_2$-group.

present study, the scheme also includes $O_2NNHC(O)CH_2OH$, *N*-nitro hydroxyacetamide, which is the expected oxidation product of $O_2NNHCH_2CH_2OH$, 2-(*N*-nitroamino)-ethanol.

According to the theoretical photo-oxidation mechanism the major pathway of the amino radical, $HNCH_2CH_2OH$, leads to the formation of $HN=CH-CH_2OH$ (2-imino ethanol, CAS: 724427-16-1 (Z), 724427-18-3 (E)). It is stressed that the fate of $HN=CHCH_2OH$ is unknown and that virtually nothing is known about the atmospheric chemistry of imines. Imines are known to hydrolyse resulting in an amine (or ammonia) and a ketone or aldehyde. In the present case, hydrolysis of $NH=CH-CH_2OH$ on chamber/inlet surfaces may give NH_3 and $CHO-CH_2OH$ (glycolaldehyde) which were both detected in larger amounts than normally expected for chamber and measurement artefacts.

The observation of $NH=CH-CH_2OH$ may also be prevented by analytical problems. One may speculate that $HN=CHCH_2OH$ will react like glycolaldehyde in contact with 2,4-dinitrophenylhydrazine and therefore be trapped on DNPH cartridges as if the parent molecules had been glycolaldehyde. We note that rather large amounts of glycolaldehyde have been detected in the DNPH cartridges. One may also speculate that $HN=CHCH_2OH$ will react with H_3O^+ in the PTR ionisation chamber to form protonated glycolaldehyde and/or protonated ammonia (reactions 23 and 24). Quantum chemistry calculations of the thermochemistry (G3 model chemistry)[42] predict that both reaction pathways are exothermic. At the present status of knowledge it is unclear if, and to which extent these reactions do occur. The PTR-TOF-MS detected only small amounts of m/z 60.044 ions which may be assigned to protonated 2-imino ethanol and/or protonated amino acetaldehyde. H_4N^+ and $C_2H_5O_2^+$ ions were observed in higher abundances and they may, at least in part, arise from $HN=CHCH_2OH$.

$$\Delta_r H_{298} = -20 \text{ kJ mol}^{-1} \quad H_2O + HN=CHCH_2OH \longrightarrow HOCH_2-CHO + NH_3 \quad (22)$$

$$\Delta_r H_{298} = -81 \text{ kJ mol}^{-1} \quad H_3O^+ + HN=CHCH_2OH \longrightarrow HOCH_2-CH(OH)^+ + NH_3 \quad (23)$$

$$\Delta_r H_{298} = -186 \text{ kJ mol}^{-1} \qquad\qquad\qquad \longrightarrow HOCH_2-CHO + NH_4^+ \quad (24)$$
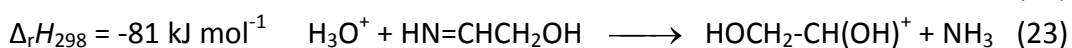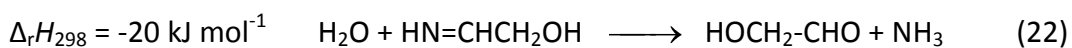
4 Aerosol model and mass balance

A new size-resolved aerosol dynamics model, MAFOR (**M**arine **A**erosol **For**mation model),[43] that is primarily designed to study aerosol evolution in the marine boundary layer has been further developed to simulate chamber experiments on photo-oxidation of amines. Implemented aerosol processes are the same as in the monodisperse aerosol dynamics model MONO32.[44-46] Several sensitivity tests have been performed to test the functionality of the model. MAFOR has been thoroughly evaluated by comparison both with simulation results from MONO32 and with field measurements.

MAFOR has been extended in the frame of the ADA project in order to include:

1) chamber specific losses of gases and particles,
2) chamber specific sources,
3) monitored time series of NO, NO_2, $j(NO_2)$, and temperature,
4) amine photo-oxidation chemistry,
5) condensation of a low-volatile MEA oxidation product to existing particles,
6) condensation of MEA-HNO_3 to existing particles, and
7) nucleation of MEA-HNO_3 particles

In the following, the model is described with focus on the new developments with respect to amine chemistry. Model simulations together with estimates of the MEA mass balance from several experiments in May 2009 are presented.

4.1 Aerosol composition during the photo-oxidation of MEA

Results are presented for the May 11 experiment. Figure 4.1 shows the composition of the aerosol at 13:01 local time (LT) (Figure 4.1b) is compared to the composition of the pure ethanolammonium salt (Figure 4.1a). Despite the similarity of the two spectra, significant differences are observed for the m/z peaks at 18, 28, 29, and 45. Without further confirmation by analysis of the particle filters the identity of the salt particles cannot be firmly concluded. It can be speculated that ethanolammonium nitrate was initially formed and then further transformed since the particles contain other salts. In a first approximation, the salt is treated as ethanolammonium nitrate in the model. The stoichiometric salt contains a smaller fraction of nitrate than what was observed in the chamber experiment. This could be due to the experimental condition (high NO_x) and/or due to possible (co-)condensation of HNO_3 or NH_4NO_3 during the experiment.

Mass peaks (m/z) above 65 in the AMS spectra are shown in Figure 4.1c. High molecular weight organics consisting of C3 and C4 fragments are detected in this part of the spectra. The contribution of these fragments to the overall particle mass is however much lower than the contribution of masses lower than m/z 65. The fraction of high molecular weight organics increased throughout the course of the experiment, but contributes only 1.1% of the total aerosol mass at 16:32 LT, short before the end of the experiment. The measured fraction is a lower limit due to the high fragmentation of the organics fraction in the AMS. Results of Murphy et al.[47] indicate that the mass yield of non-salt aerosol during photo-

oxidation experiments with aliphatic amines is in general low. For the photo-oxidation of MEA the mass-based yield of non-salt particles was reported to be only 2%. [47]
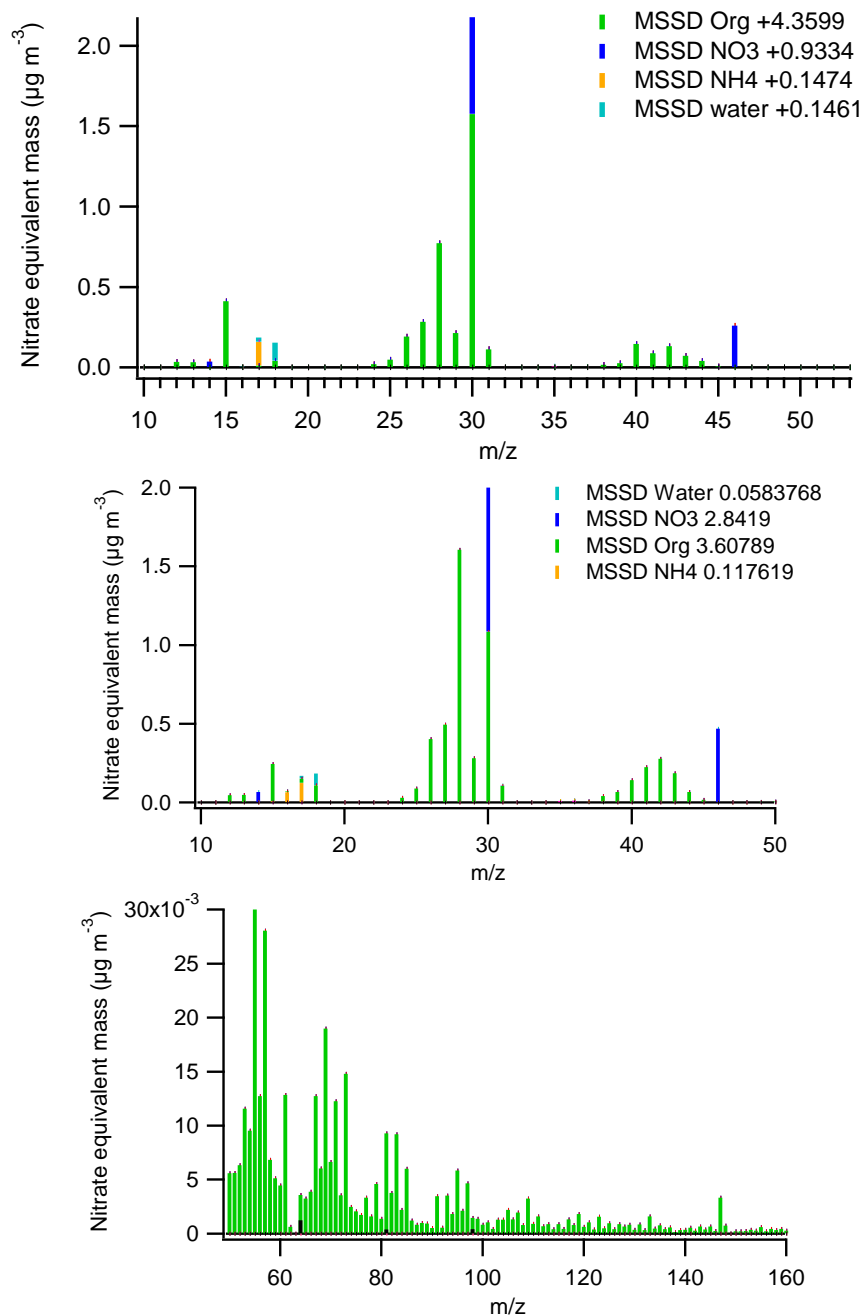
Figure 4.1. AMS spectra of a) the pure (stoichiometric) ethanolammonium nitrate salt, b) the aerosol obtained during the photo-oxidation experiment at 13:01 local time (m/z lower than 55), and c) the high molecular weight organic fragments at the same time (m/z higher than 55). Data from the May 11 experiment.

An unexpected contribution of ammonium (NH_4^+) was detected by AMS in the aerosol at 16:32 local time. We speculate that ammonium condensed to the existing particles in the form of ammonium nitrate. The contribution of the ammonium mass to the total aerosol mass remained below 2% during the experiment.

4.2   Mass balance of MEA during the photo-oxidation of MEA

The experiments in the ADA campaign were designed to study the degradation of MEA in the gas phase. After MEA is added to the chamber volume in the dark, several processes can contribute to the overall decay of the MEA concentration during an experiment. MEA is rapidly lost to the walls and also undergoes loss by the replenishment flow which dilutes the concentrations of all long-lived compounds in the chamber. After the chamber is exposed to sunlight, the OH-initiated oxidation of MEA can start and MEA is to a large extent degraded by chemical reaction with the OH radical. However, substantial amounts of the injected MEA amount are converted into particle mass (gas-to-particle conversion) during the photo-oxidation experiments. We assume, that this occurs in first line by nucleation of new particles consisting of ethanolammonium nitrate. In later steps of the experiments also condensation of MEA-HNO$_3$ to existing particles takes place. In the MEA photo-oxidation experiments several thousands of new particles form per cubic centimetre. The newly generated particles grow fast from sizes of 18 nm (and below) to 100 nm or larger. An example for the temporal evolution of the aerosol size distribution is shown in Figure 4.2.

The measured concentration time series of MEA can thus not only be explained by the chemical reaction of MEA with OH. Application of a box model becomes necessary to describe how the respective loss processes contribute to the overall
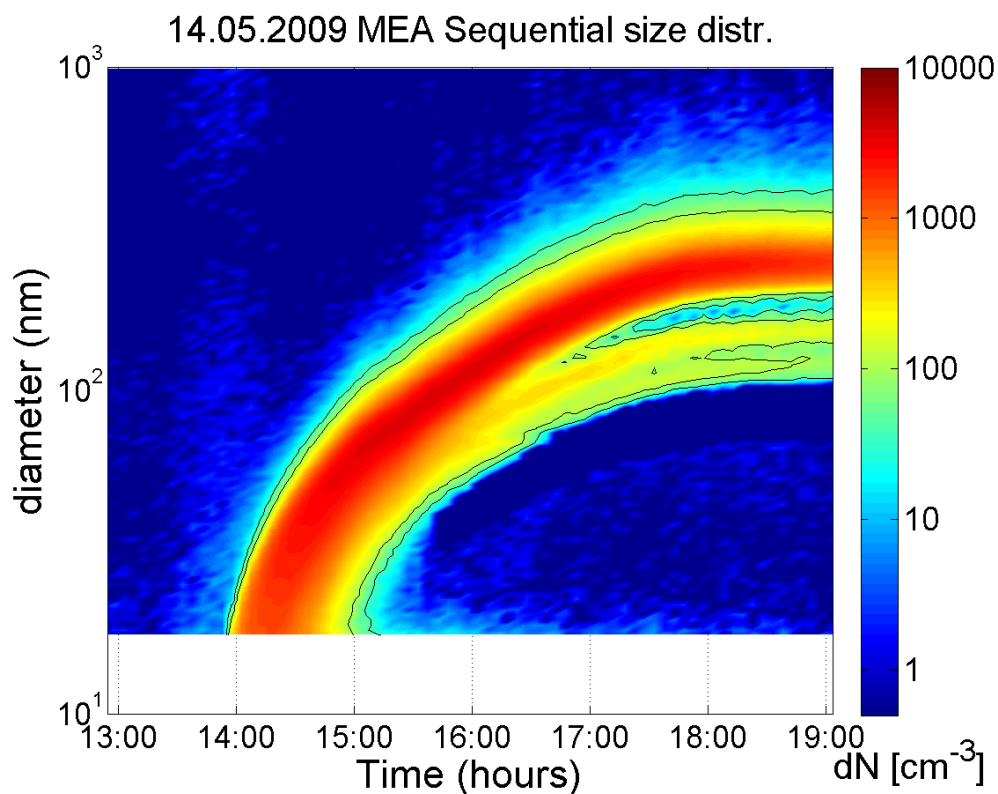
Figure 4.2. Sequential size distributions in the MEA photo-oxidation experiment on 14.05.2009. Time is given as local time. A particle burst is observed one hour after the chamber roof was opened at 12:56. Lower size cut-off of the SMPS instrument is at 17.5 nm diameter.

degradation of MEA. MAFOR includes both the gas phase chemistry scheme (photochemistry) and the aerosol dynamic processes. Model simulations were performed for the photo-oxidation experiments on May 10, 11, 14 and 15 to determine the mass balance of MEA. In all simulations four fit parameters were varied to obtain the best agreement between modelled and measured time series of MEA, formamide, total aerosol load and total number concentration. Two scenarios were studied: in the first initial MEA concentration measured by PTR-MS or FT-IR instrument is used to initialize the model, and in the second the MEA concentration of the first filter sample analyzed by LC-MS is used to initialize the model. Both model simulation allow to conclude about the mass closure of MEA in the experiment and the percentage fraction of each loss process is provided for both scenarios. In the following, only the first scenario is discussed in more detail.

In the experiment on May 11, MEA was added into the dark chamber between 09:07 and 09:45 local time (LT). At 10:57 LT, NO was injected and at 12:48 the chamber roof was opened. Immediately at 12:52 a particle burst was observed. The chamber was closed at 16:39. The time when the chamber was exposed to sunlight defines the period and duration of the experiment. Figure 4.3 shows the measured and modelled time series. The modelled time series is shown for the first three hours of the sunlit period because in later stages of the experiment particle processes occurred which cannot be reproduced by the model (e.g. oxidation on particles or condensation of SOA). Measured and modelled ozone concentrations were below 10 ppbv (Figure 4.3a).

Measured time series of MEA and formamide are reproduced by the model (Figure 4.3b). Formamide is the major oxidation product of MEA with a product yield of 0.8. Total aerosol mass load has been measured with three instruments: SMPS, AMS, and TEOM. Measurements with TEOM have the lowest accuracy and were not used here.

The two aerosol instruments, SMPS and AMS, measure different types of aerosol diameter. AMS measures an aerodynamic diameter by acceleration in the vacuum, while SMPS measures the mobility diameter. SMPS measures the aerosol at a density of $1000 \, \text{kg m}^{-3}$ (unit density). By comparison of AMS and SMPS mass loadings, the particle density during the experiment can be derived. In general, particle densities of about $1300 \, \text{kg m}^{-3}$ were found in the experiments. The particle mass concentration measured by SMPS was then corrected with the derived particle density ($1300 \, \text{kg m}^{-3}$). The model curve was adjusted to the slope and magnitude of the AMS total mass curve (blue squares in Figure 4.3c). Measured mass fractions of MEA and nitrate in the aerosol are almost equally large and only a small fraction is from high-molecular weight organics and ammonium. The two latter aerosol constituents increase with experiment time but remain below 2% of the total aerosol mass. In the first two hours good agreement between modelled and measured (AMS) total particle mass concentration was achieved. The shift of the particle number size distribution to higher diameters and the increase in number concentration (Figure 4.3d) could not be fully reproduced. The reason for this deviation could be the parameterization of the condensation process in the aerosol model.

Another reason could be that the size-dependent parameterization of the wall loss of particles in the chamber does not correctly reproduce the particle loss in EUPHORE. The parameterization is according to Naumann[48] and takes into account the geometry of the EUPHORE chamber. The gas phase concentration of MEA and formamide are well reproduced by the model, indicating that available MEA vapour was properly converted into particle bound MEA.
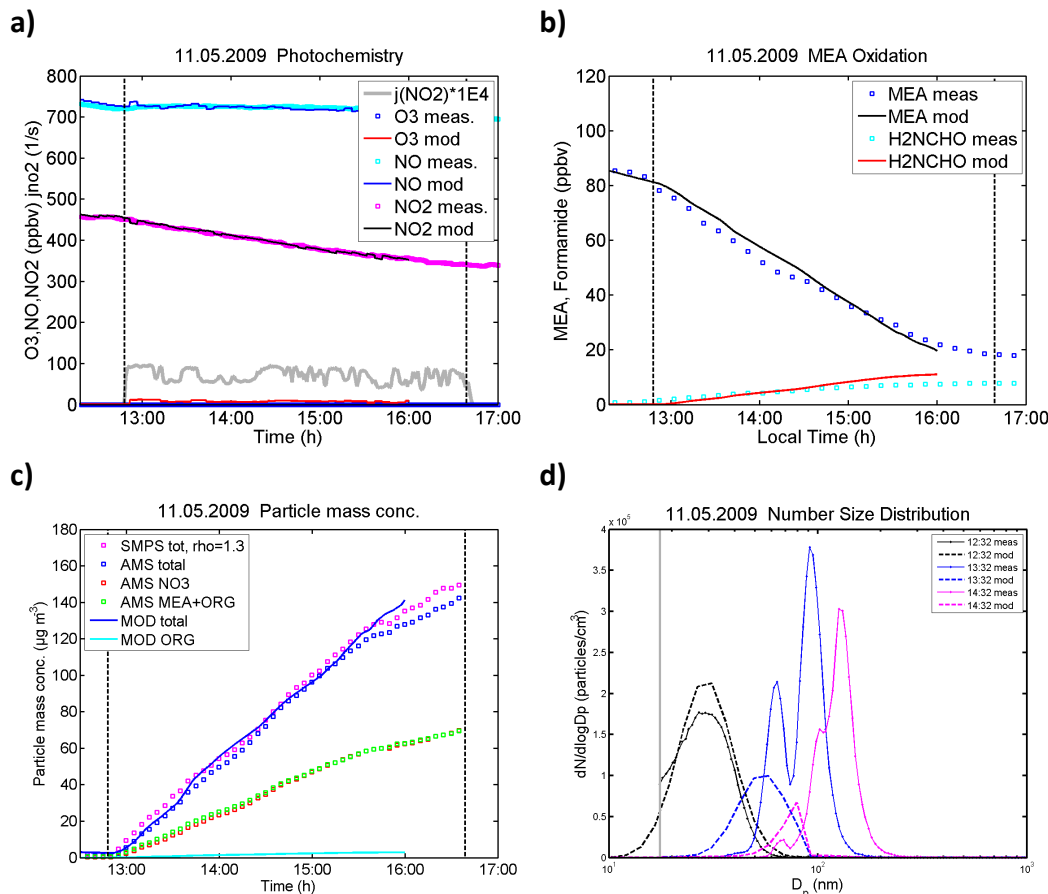
Figure 4.3. Measured and modelled (best fit) time series of the MEA experiment on 11.05.2009. a) concentrations of NO, NO_2, and O_3 in ppbv and photolysis frequency of NO_2 (scaled by $1x10^4$) in s^{-1}, b) concentrations of MEA and formamide measured by PTR-MS and modelled, c) total particle mass concentration (in $\mu g\ m^{-3}$) measured by AMS (blue squares), SMPS (magenta squares) and modelled (blue line), d) particle number size distribution (dN/dlogDp) measured with SMPS (line with points) and from model output (dashed line) at 12:32 (black), 13:32 (blue), and 14:32 (magenta). Time is given as local time. The time period between the vertical lines is the sunlit experiment.

To study the mass balance of MEA during the experiment, two additional simulations were performed with the same model configuration: one simulation in which MEA was only depleted by reaction with OH (*i.e.* no conversion into particles, wall loss or dilution) and one simulation in which the wall loss of MEA was neglected while all other processes were included. The resulting model MEA concentrations are displayed in Figure 4.4.

In Figure 4.4, the difference between the simulation with all processes (dashed line) and the simulation without wall loss (dotted line) corresponds to the

fraction of MEA wall loss. The difference between the simulation without wall loss and the simulation with only chemistry (dash-dotted line) corresponds to the fraction of MEA converted to particles. The difference between the simulation with only chemistry and the initial MEA concentration (thin solid line) corresponds to the fraction of MEA reacted.
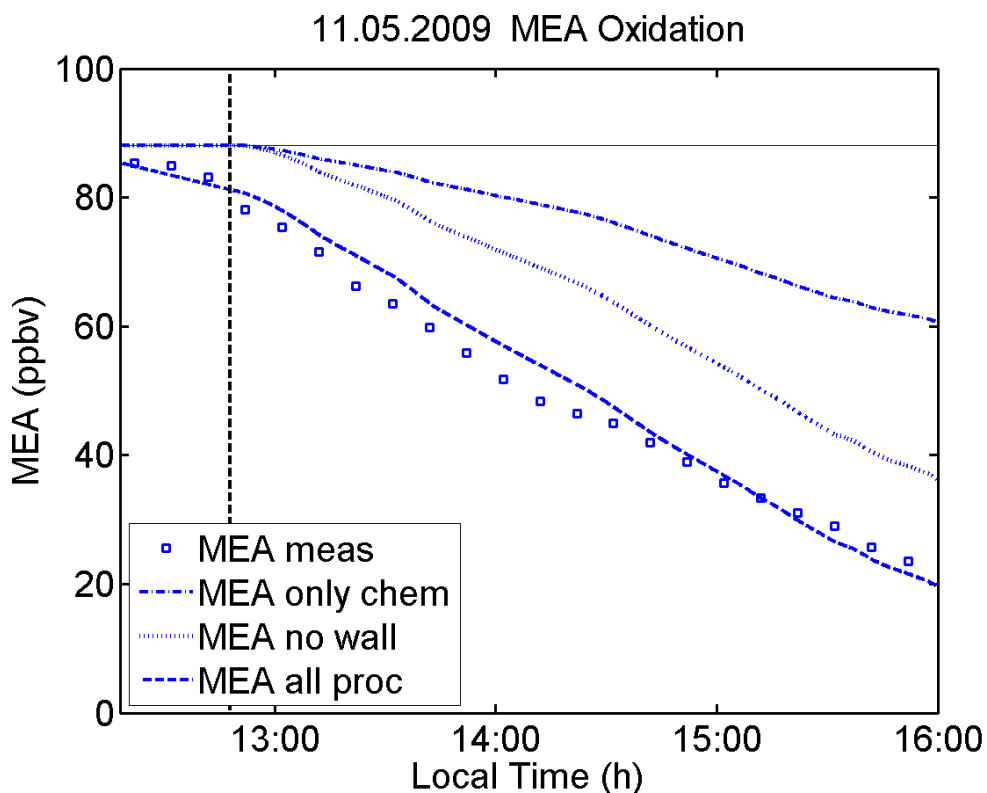
Figure 4.4. Mass balance of MEA during the experiment on May 11. MEA concentration measured (squares), from standard simulation with all processes active (dashed line), from simulation without wall loss and dilution (dotted line), and from simulation with only depletion by chemical reaction (dash-dotted line). Thin solid line indicates mass balance of 100%.

5 Ozone formation potential

The formation of ozone during the photochemical oxidation of MEA was studied in the experiment on May 15, and September 10 and 11. The current experiments revealed that MEA is an efficient ozone precursor. In short, the relative behaviour of VOCs and NOx in ozone formation can be understood in competition for the OH radical. In the photo-oxidation experiments with an initial MEA-to-NO_2 ratio of less then 5.5:1, OH reacts predominantly with NO_2 to give nitric acid, by which radicals are removed and thus ozone formation is slowed down.
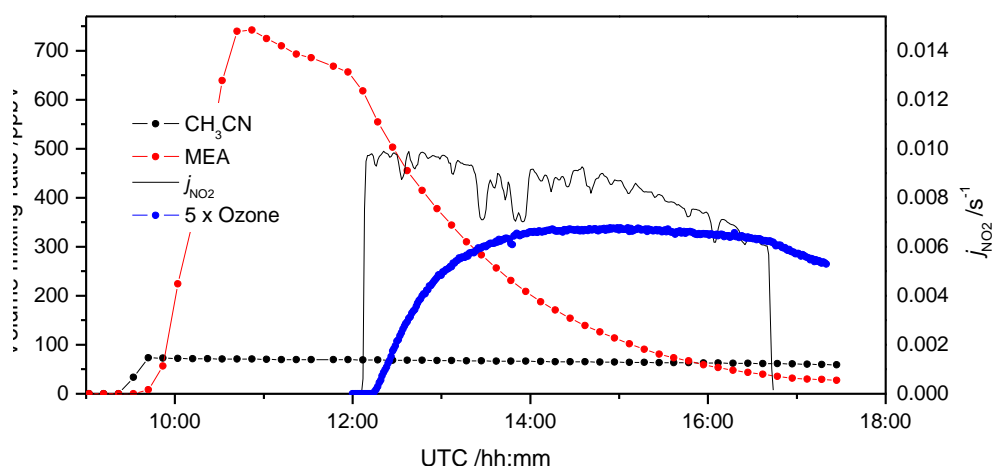
Figure 5.1. Investigation of the ozone formation potential of MEA. Photolysis frequency of NO_2, j_{NO2}, and the time evolution of MEA, O_3 (scaled by a factor of 5) and acetonitrile during the photo-oxidation experiment on May 15.

Optimum conditions for ozone production in MEA photo-oxidation experiments are 1) high actinic flux (high j_{NO2}), and 2) initial MEA-to-NO_x ratio >5.5, for example 500 ppbv MEA and 80 ppbv NO_2 or NO. During most experiments in May, the MEA-to-NO_x ratio was below 1. In the experiment on May 15, the initial MEA concentration was about 500 ppbv, initial NO was about 30 ppbv, and the photolysis frequency of NO_2 was close to 0.010 s^{-1}. Rapid ozone formation was observed and ozone concentrations reached ~70 ppbV during the experiment. Model calculation showed that in this experiment approximately 70 ppbv MEA was depleted by reaction with OH radicals. Using the monitored time series of ozone and the simulated chemical degradation of MEA, the ozone formation potential defined as $\Delta O_3/\Delta MEA_{reac}$ was found to be ~1 during the first 2.5 hours of the experiment. This finding implies that each molecule of MEA reacted produces one molecule of ozone. Consequently, MEA is an efficient ozone producer and its ozone formation potential is comparable to that of acetaldehyde. The present result confirms the recently reported ozone formation potential of MEA.[49]

6 Conclusions from the photo-oxidation studies

The photo-oxidation of MEA has been studied in two campaigns at the European Photochemical Reactor, EUPHORE, in Valencia (Spain). The experimental day to day conditions have spanned a wide range resulting in large differences between the gas phase removal processes (photo-oxidation, aerosol formation, wall loss).

About 20-50% of the degradation of MEA in the analyzed experiments is due the chemical reaction with OH radicals (Table 6.1). A substantial fraction of MEA, about 10-40% is converted into particles. About 30-70% of the initial MEA amount is lost to the walls or by dilution through the replenishment flow. A good characterization of the MEA wall loss is an important prerequisite to conduct MEA experiments. The aerosol model MAFOR was demonstrated to be a useful and reliable tool for the determination of the MEA mass balance during photo-oxidation experiment. The main sources of uncertainty in the mass balance calculation are the rate constant of the OH+MEA reaction and the MEA wall loss rate.

Table 6.1. Mass balance of MEA in May experiments in percentage: chemical reaction, conversion to particulate phase and wall loss (including dilution loss). The first three hours of the sunlit experiment were used to derive the mass balance.

Date	Chemical reaction (%)	Particle conversion (%)	Wall loss (%)
10.05.2009	51	21	28
11.05.2009	31	36	33
14.05.2009	42	5	53
15.05.2009	16	13	71

The results for the mass balance given in Table 6.1 are entirely based on the available measurements from the online methods. The relative contributions to MEA losses will change when using different measurements of the MEA concentration (i.e. off-line method). For example using MEA measured by the off-line method in the experiment on May 15 would result in a relative wall loss contribution of 89% (online method: 71%) while the respective contribution of chemistry and particles would be 3-4% (online method: 13-16%). It is noted that the aerosol mass loading is less well reproduced when using MEA from off-line techniques.

The formation of secondary (non-salt) organic aerosol from the photo-oxidation of MEA was found to be small (6% or less), confirming earlier results by Murphy et al. [47]

MEA is highly water soluble with a Henry's Law coefficient of 6.2×10^6 M atm^{-1}, i.e. 5 to 6 orders of magnitude higher than that for sulphur dioxide or ammonia. Thus a large fraction of emitted amines will partition into the aqueous phase of aerosols and clouds. Uptake of MEA into liquid films occurs fast, and the humid experiment of the May campaign showed that the uptake is four times faster

than the chemical reaction with the OH radical in the gas phase in the chamber. In the atmospheric boundary layer wetted surfaces (buildings, particles, cloud droplets) are present which will provide a medium for the uptake of MEA. Dispersion model calculations including the gas phase/liquid phase partitioning of MEA are necessary to decide, if the loss process is relevant.

The lifetime of amines in (bulk) water is expected to be in the range of 14 to 20 days, but experimental evidence on the chemical transformation of amines and its degradation products in water is lacking. For the fate of amines in aerosols and clouds it is of great importance to know about their reaction rates with OH (OH_{aq}) in the aqueous phase. Assuming a aqueous phase reaction rate with the aqueous OH radical similar to that of ethanol, the lifetime of dissolved MEA in cloud droplets in an remote environment ([OH]=$1x10^{-6}$ molec cm^{-3}) would be only 0.1 hours. In addition it is known that solutions of amines are basic and thus emissions of amines will impact the pH of cloud and rain droplets. Amines efficiently lower the surface tension of water droplets and thereby facilitate the growth of aerosols.[50]

Results from modelling the observed product distribution in the four experiments are summarized in Table 6.2. Considering the very different experimental conditions the derived branching ratios have an acceptable scatter and a conservative statement will be that the branching ratios in the OH initiated H-abstraction from NH_2-CH_2-CH_2OH are: <10 % from -NH_2, >80 % from –CH_2– , and <10 % from -CH_2OH. It is stressed, again, that the branching ratio k_4/k_{tot} is an upper limit.

Table 6.2. Branching ratios in the $NH_2CH_2CH_2OH$ reaction with OH radicals inferred from observed product distribution..

Date	$(k_1 + k_2)/k_{tot}$	k_3/k_{tot}	k_4/k_{tot}
10.05.2009	0.08	0.80	0.12
11.05.2009	0.05	0.87	0.08
14.05.2009	0.06	0.83	0.07
15.05.2009	0.12	083	0.05
Average	0.08 ± 0.03	0.84 ± 0.03	0.08 ± 0.03

The major products in the photo-oxidation are formamide and formaldehyde. The latter has a short atmospheric lifetime and undergoes photolysis or reacts fast with OH radicals. Minor products are amino acetaldehyde and 2-oxo acetamide. The former will have a relative short atmospheric lifetime. The product yield of the nitramine, $O_2NNHCH_2CH_2OH$, varies among the experiments from 3 ‰ to 1.5 % depending on the NOx-level in the experiment.

The major product resulting from hydrogen abstraction from the NH_2-group is, according to the chemistry model, the imine, $HN=CH_2CH_2OH$. The atmospheric chemistry of this compound is unknown and it has not been detected unambiguously by any of the available analytical instrumentation or off-line methods. Essentially 8 ± 3 % of the mass is therefore unaccounted for in the experiments for this reason alone. The quantification of amino acetaldehyde and

2-oxo acetamide is very tentative (there are no standards available) and this places a conservative upper limit to the mass unaccounted for to 16 %.

The amount of $O_2NNHCH_2CH_2OH$ formed during photo-oxidation of MEA emitted to the atmosphere depends on the mixing ratio of NOx. Typical mixing ratios of NOx are 10-1000 ppbV (suburban-urban) and 0.2-10 ppbV (rural).[51] A realistic US and West European urban scenario will have NOx around 50 ppbV, and with an average ratio $NO:NO_2 = 1:2$, the molar yield of $O_2NNHCH_2CH_2OH$ from MEA photo-oxidation is predicted to be 3-10 ‰ in urban regions and 0.05-3 ‰ in rural regions.

7 ADA Protocol for amine screening studies

MEA is often considered a benchmark solvent for post combustion CO_2 capture. The atmospheric photo-oxidation of MEA was studied under varying conditions to find branching ratios in the initial hydrogen abstraction by OH radicals and to identify all major products in the oxidation of MEA emitted to the atmosphere. Compounds of special interest in this context were the nitrosamine ($ONNHCH_2CH_2OH$) and the nitramine ($O_2NNHCH_2CH_2OH$).

The various photo-oxidation studies carried out at the EUPHORE facility over a 3-week period in May 2009 and during a 1-week period in September 2009 were subsequently analysed not only to extract the abovementioned kinetic and mechanistic information. The experiments were also analysed with the aim to extract a cost-efficient Experiment Protocol for amine screening studies as part of an environmental impact assessment.

The suggested Experiment Protocol defines a series of photo-oxidation experiments which are suited to elucidate the fate of amines emitted to the atmosphere. The Protocol focuses on the identification of malevolent compounds and includes some requirements to be met by the experiments.

1. Documentation of instrumentation and methodologies.
  1. Instrumentation and analytical methodologies should be documented in agreement with practice in international journals of atmospheric and analytical chemistry.
  2. Documentation of transfer lines between chamber and on-line and off-line instruments and sampling devices.
  3. Documentation of spectral distribution and intensity of photolysis source.
  4. Documentation of the chamber injection system.

2. Minimum requirements of experiment analysis.
  1. All loss processes (surface, particles, gas-phase photo-oxidation) should be quantified and models documented in agreement with practice in international atmospheric chemistry journals. The amount of amine removed by gas-phase photo-oxidation should exceed 100 ppbV.
  2. Mass closure > 80 %.

3. Specific chemical tests (Target analysis).
  1. Test for *N*-nitrosamines in the gas phase and aerosol. LoD ~10 pptV (10^{-4} of amine removed in gas-phase photo-oxidation).
  2. Test for *N*-nitramines in the gas phase and aerosol. LoD ~1 ppbV achieved during ADA (10^{-2} of amine removed in gas-phase photo-oxidation).
  3. Test for *N*-Nitro amides in the gas phase and aerosol. Not available yet.
  4. Test for carbonyl compounds.

4. Recommended experiment conditions.

1. High-NO$_x$ experiment (dry air, high actinic flux): 200-500 ppb amine, 80 ppb NO, 160 ppb NO$_2$. If possible, continuous addition of NO/NO$_2$ to keep NO$_x$ constant throughout the experiment.
2. Low-NO$_x$ experiment (dry air, high actinic flux): 200-500 ppb amine, 10 ppb NO, 20 ppb NO$_2$. If possible, continuous addition of NO/NO$_2$ to keep NO$_x$ constant throughout the experiment.
3. High-NO$_x$ experiment (dry air, dark conditions): 200-500 ppb amine, 80 ppb NO, 160 ppb NO$_2$. If possible, continuous addition of NO/NO$_2$ to keep NO$_x$ constant throughout the experiment.

5. Other quantities to be reported

1. Ozone formation potential, $\Delta[O_3]/\Delta[Amine]_{reacted}$.
2. Quantification of the particle production yield using measured particle mass loading.

8   Literature

(1)   Bråten, H.B., Bunkan, A.J., Bache-Andreassen, L., Solimannejad, M. and Nielsen, C.J. (2008) Final report on a theoretical study on the atmospheric degradation of selected amines. Kjeller, Norwegian Institue for Air Research (NILU OR 77/2008).

(2)   Carter, W.P.L. and Atkinson, R. (1985) Atmospheric chemistry of alkanes. *J. Atmos. Chem., 3*, 377-405.

(3)   Atkinson, R. (1986) Kinetics and mechanisms of the gas-phase reactions of the hydroxyl radical with organic-compounds under atmospheric conditions. *Chem. Rev., 86*, 69-201.

(4)   Atkinson, R., Perry, R.A. and Pitts, J.N., Jr. (1977) Rate constants for the reaction of the hydroxyl radical with methanethiol and methylamine over the temperature range 299-426 DegK. *J. Chem. Phys., 66*, 1578-1581.

(5)   Carl, S.A. and Crowley, J.N. (1998) Sequential two (blue) photon absorption by NO2 in the presence of H2 as a source of OH in pulsed photolysis kinetic studies: Rate constants for reaction of OH with CH3NH2, (CH3)2NH, (CH3)3N, and C2H5NH2 at 295 K. *J. of Phys. Chem. A, 102*, 8131-8141.

(6)   Atkinson, R., Perry, R.A. and Pitts, J.N., Jr. (1978) Rate constants for the reaction of hydroxyl radicals with carbonyl sulfide, carbon disulfide and dimethyl thioether over the temperature range 299-430 K. *Chem. Phys. Lett., 54*, 14-18.

(7)   Gorse, R.A., Jr., Lii, R.R. and Saunders, B.B. (1977) Hydroxyl radical reactivity with diethylhydroxylamine. *Science, 197*, 1365-1367.

(8)   Harris, G.W. and Pitts, J.N. (1983) Rates of reaction of hydroxyl radicals with 2-(dimethylamino)ethanol and 2-amino-2-methyl-1-propanol in the gas-phase at 300 +- 2 K. *Environ. Sci. Technol., 17*, 50-51.

(9)   Anderson, L.G. and Stephens, R.D. (1988) Kinetics of the reaction of hydroxyl radicals with 2-(dimethylamino)ethanol from 234-364-K. *Int. J. Chem. Kinet., 20*, 103-110.

(10)   Koch, R., Kruger, H.U., Elend, M., Palm, W.U. and Zetzsch, C. (1996) Rate constants for the gas-phase reaction of OH with amines: tert-butyl amine, 2,2,2-trifluoroethyl amine, and 1,4-diazabicyclo[2.2.2]octane. *Int. J. Chem. Kinet., 28*, 807-815.

(11)   Pitts, J.N., Grosjean, D., Vancauwenberghe, K., Schmid, J.P. and Fitz, D.R. (1978) Photo-oxidation of aliphatic-amines under simulated atmospheric conditions - Formation of nitrosamines, nitramines, amides, and photo-chemical oxidant. *Environ. Sci. Technol., 12*, 946-953.

(12)   Lindley, C.R.C., Calvert, J.G. and Shaw, J.H. (1979) Rate studies of the reactions of the (CH3)2N radical with O2, NO, and NO2. *Chem. Phys. Lett., 67*, 57-62.

(13)   Tuazon, E.C., Atkinson, R., Aschmann, S.M. and Arey, J. (1994) Kinetics and products of the gas-phase reactions of O3 with amines and related-compounds. *Res. Chem. Intermed., 20*, 303-320.

(14)   Tuazon, E.C., Carter, W.P.L., Atkinson, R., Winer, A.M. and Pitts, J.N. (1984) Atmospheric reactions of N-nitrosodimethylamine and dimethylnitramine. *Environ. Sci. Technol., 18*, 49-54.

(15) Tuazon, E.C., Winer, A.M., Graham, R.A., Schmid, J.P. and Pitts, J.N. (1978) Fourier-transform infrared detection of nitramines in irradiated amine-NOx systems. *Environ. Sci. Technol., 12*, 954-958.

(16) Pitts, J.N., Smith, J.P., Fitz, D.R. and Grosjean, D. (1977) Enhancement of photochemical smog by N, N'-diethylhydroxylamine in polluted ambient air. *Science, 197*, 255-257.

(17) Grosjean, D. (1980) Atmospheric chemistry of selected nitrogenous pollutants. *Calif. Air Environ., 7*, 12-15.

(18) Grosjean, D. (1991) Atmospheric chemistry of toxic contaminants. 6. nitrosamines: dialkyl nitrosamines and nitrosomorpholine. *J. Air Waste Manage. Assoc. (1990-1992), 41*, 306-311.

(19) Geiger, G. and Huber, J.R. (1981) Photolysis of dimethylnitrosamine in the gas-phase. *Helv. Chim. Acta, 64*, 989-995.

(20) Drewnick, F., Hings, S., Decarlo, P., Jayne, J., Gonin, M., Fuhrer, K., Weimer, S., Jimenez, J., Demerjian, K., Borrmann, S. and Worsnop, D. (2005) A new time-of-flight aerosol mass spectrometer (TOF-AMS) - instrument description and first field deployment. *Aerosol Sci. Technol., 39*, 637-658.

(21) Favez, O., El Haddad, I., Piot, C., Boréave, A., Abidi, E., Marchand, N., Jaffrezo, J.-L., Besombes, J.-L., Personnaz, M.-B., Sciare, J., Wortham, H., George, C. and D'anna, B. (2010) Inter-comparison of source apportionment models for the estimation of wood burning aerosols during wintertime in an Alpine city (Grenoble, France). *Atmos. Chem. Phys. Discuss., 10, 559-613.*

(22) Griffith, D.W.T. (1996) Synthetic calibration and quantitative analysis of gas-phase FT-IR spectra. *Appl. Spectrosc., 50*, 59-70.

(23) Rothman, L.S., Gordon, I.E., Barbe, A., Chrisbenner, D., Bernath, P.F., Birk, M., Boudon, V., Brown, L.R., Campargue, A., Champion, J.-P., Chance, K., Coudert, L.H., Danaj, V., Devi, V.M., Fally, S., Flaud, J.-M., Gamache, R.R., Goldmanm, A., Jacquemart, D., Kleiner, I., Lacome, N., Lafferty, W.J., Mandin, J.-Y., Massie, S.T., Mikhailenko, S.N., Miller, C.E., Moazzen-Ahmadi, N., Naumenko, O.V., Nikitin, A.V., Orphal, J., Perevalov, V.I., Perrin, A., Predoi-Cross, A., Rinsland, C.P., Rotger, M., Simeckova, M., Smith, M.A.H., Sung, K., Tashkun, S.A., Tennyson, J., Toth, R.A., Vandaele, A.C. and Vanderauwera, J. (2009) The HITRAN 2008 molecular spectroscopic database. *J. Quant. Spectrosc. Radiat. Transfer, 110*, 533-572.

(24) Becker, K.H. (1996) The European photoreactor EUPHORE. Design and technical development of the European photoreactor and first experimental results. Final report of the EC-project contract (EV5V-CT92-0059). Wuppertal, BUGH Wuppertal.

(25) Magneron, I., Thevenet, R., Mellouki, A., Le Bras, G., Moortgat, G.K. and Wirtz, K. (2002) A study of the photolysis and OH-initiated oxidation of acrolein and trans-crotonaldehyde. *J. Phys. Chem. A, 106*, 2526-2537.

(26) Volkamer, R., Platt, U. and Wirtz, K. (2001) Primary and secondary glyoxal formation from aromatics: Experimental evidence for the bicycloalkyl-

radical pathway from benzene, toluene, and p-xylene. *J. Phys. Chem. A, 105*, 7865-7874.

(27) Klotz, B., Sorensen, S., Barnes, I., Becker, K.H., Etzkorn, T., Volkamer, R., Platt, U., Wirtz, K. and Martin-Reviejo, M. (1998) Atmospheric oxidation of toluene in a large-volume outdoor photoreactor: In situ determination of ring-retaining product yields. *J. Phys. Chem. A, 102*, 10289-10299.

(28) Wenger, J.C., Le Calve, S., Sidebottom, H.W., Wirtz, K., Reviejo, M.M. and Franklin, J.A. (2004) Photolysis of chloral under atmospheric conditions. *Environ. Sci. Technol., 38*, 831-837.

(29) Mascavage, L.M., Sonnet, P.E. and Dalton, D.R. (2006) On the surface-catalyzed reaction between the gases 2,2-dimethylpropanal and methanamine. Formation of active-site imines. *J. Org. Chem.y, 71*, 3435-3443.

(30) Takahashi, N. and Katsuki, O. (1990) Decomposition of ethylene glycol by the combined use of ozone oxidation and electrolytic methods. *Ozone: Sci. Eng., 12*, 115-131.

(31) D'anna, B., Bakken, V., Beukes, J.A., Nielsen, C.J., Brudnik, K. and Jodkowski, J.T. (2003) Experimental and theoretical studies of gas phase NO3 and OH radical reactions with formaldehyde, acetaldehyde and their isotopomers. *Phys. Chem. Chem. Phys., 5*, 1790-1805.

(32) Feilberg, K.L., Johnson, M.S. and Nielsen, C.J. (2004) Relative reaction rates of HCHO, HCDO, DCDO, (HCHO)-C-13, and (HCHO)-O-18 with OH, Cl, Br, and NO3 radicals. *J. Phys. Chem. A, 108*, 7393-7398.

(33) Feilberg, K.L., D'anna, B., Johnson, M.S. and Nielsen, C.J. (2005) Relative tropospheric photolysis rates of HCHO, (HCHO)-C-13, (HCHO)-O-18, and DCDO measured at the European photoreactor facility. *J. Phys. Chem. A, 109*, 8314-8319.

(34) Nilsson, E.J.K., Bache-Andreassen, L., Johnson, M.S. and Nielsen, C.J. (2009) Relative tropospheric photolysis rates of acetaldehyde and formaldehyde isotopologues measured at the European photoreactor facility. *J. Phys. Chem. A, 113*, 3498-3504.

(35) Bone, R., Cullis, P. and Wolfenden, R. (1983) Solvent effects on equilibria of addition of nucleophiles to acetaldehyde and the hydrophilic character of diols. *J. Am. Chem. Soc., 105*, 1339-1343.

(36) Svensson, R., Ljungstrom, E. and Lindqvist, O. (1987) Kinetics of the reaction between nitrogen-dioxide and water-vapor. *Atmos. Environ., 21*, 1529-1539.

(37) Tang, I.N. and Munkelwitz, H.R. (1994) Water activities, densities, and refractive indices of aqueous sulfates and sodium nitrate droplets of atmospheric importance. *J. Geophys. Res. Atmos., 99*, 18,801-808.

(38) Schwartz, S.E. (1986) Mass transport considerations pertinent to aqueous phase reactions of gases in liquid water clouds. In: *Chemistry of multiphase atmospheric systems.* Ed. by: Jaeschke, W. Berlin, Springer (NATO ASI Series, Series G, Ecological sciences, 6). pp. 415-471.

(39) IUPAC Subcommittee for Gas Kinetic Data Evaluation (2009) URL: http://www.iupac-kinetic.ch.cam.ac.uk/index.html

(40)   Atkinson, R., Perry, R.A. and Pitts, J.N., Jr. (1978) Rate constants for the reactions of the hydroxyl radical with dimethylamine, trimethylamine, and ethylamine over the temperature range 298-426 K. *J. Chem. Phys., 68*, 1850-1853.

(41)   Lazarou, Y.G., Kambanis, K.G. and Papagiannakopoulos, P. (1994) Gas-phase reactions of (CH3)2N radicals with NO and NO2. *J. Phys. Chem., 98*, 2110-2115.

(42)   Curtiss, L.A., Raghavachari, K., Redfern, P.C., Rassolov, V. and Pople, J.A. (1998) Gaussian-3 (G3) theory for molecules containing first and second-row atoms. *J. Chem. Phys., 109*, 7764-7776.

(43)   Karl, M., Gross, A., Pirjola, L. and Leck, C. (2009) Testing different nucleation schemes to simulate new particle formation in the High Arctic. *(Manuscript in preparation).*

(44)   Pirjola, L. and Kulmala, M. (2000) Aerosol dynamical model MULTIMONO. *Boreal Environ. Res., 5*, 361-374.

(45)   Pirjola, L., Tsyro, S., Tarrason, L. and Kulmala, M. (2003) A monodisperse aerosol dynamics module, a promising candidate for use in long-range transport models: Box model tests. *J. Geophys. Res. Atmos., 108, D9,* 4258.

(46)   Karl, M., Gross, A., Leck, C., and Pirjola, L. (2007) Intercomparison of dimethylsulfide oxidation mechanisms for the marine boundary layer: Gaseous and particulate sulfur constituents. *J. Geophys. Res. Atmos., 112, D15304*.

(47)   Murphy, S.M., Sorooshian, A., Kroll, J.H., Ng, N.L., Chhabra, P., Tong, C., Surratt, J.D., Knipping, E., Flagan, R.C. and Seinfeld, J.H. (2007) Secondary aerosol formation from atmospheric reactions of aliphatic amines. *Atmos. Chem. Phys, 7*, 2313-2337.

(48)   Naumann, K.H. (2003) COSIMA - a computer program simulating the dynamics of fractal aerosols. *J. Aerosol. Sci., 34*, 1371-1397.

(49)   Carter, W.P.L. (2008) Reactivity estimates for selected consumer product compounds. Final report to the California Air Resources Board. Riverside, CA, Center for Environmental Research and Technology, College of Engineering, University of California.

(50)   Karl, M. (2008) Amines and rainfall. Impact of amines on rainfall from plume clouds (task 5.3). Kjeller, Norwegian Institute for Air Research (NILU OR 74/2008).

(51)   National Research Council (1991) Rethinking the ozone problem in urban and regional air pollution. Washington, D.C., National Academy Press.

58

ANNEX:
Comparison between on-line, *in situ* and off-line analytical results

60

Quality assurance for off-line methods

The NILU laboratories are equipped with highly advanced instruments, and chemical analyses and monitoring instruments have been accredited according to NS-EN ISO/IEC 17025 since 1993. All off-line analysis has been performed according to the laboratory's established quality assurance routines. The method for determination of carbonyl compounds is based on certified reference material, and the methods for amine and formamide measurements are based on highest purity reference material. All volumetric and gravimetric equipment undergoes regularly control of the accuracy. The expanded uncertainty for formaldehyde and acetaldehyde is 12% and 14 %, respectively, with a valid measure area from 1ppb to 100ppm. Typical DNPH-carbonyl limit of detection at 90 L sample volume is lower than 0.1 ppb. Glycolaldehyde is not validated and no standard were used in the quantification work. The expanded uncertainty of the amine and amid measurements is estimated to 15%, with limits of detection of 2ppb and 0.1 ppb, respectively. The limits of detection for the amine method can easily be improved by increasing the size of the filter aliquot, if necessary ppt level is reachable. In the off-line analysis the major factor in the expanded uncertainty is sampling and sample collection.

Formaldehyde, CH_2O (/ppbV)

Date	Method	Sample 1	Sample 2	Sample 3
2009.05.10	Off-line DNPH	1.87	9.88	13.18
	PTR-TOF-MS[a] m/z 31.018	2.3	23.4	22.5
	FT-IR[b]	3	12	11
2009.05.11	Off-line DNPH	1.14	7.19	13.17
	PTR-TOF-MS m/z 31.018	1.9	9.0	9.9
	FT-IR	< LoD	4	5
2009.05.14	Off-line DNPH	2.48	60.29	
	PTR-TOF-MS m/z 31.018	3.6	29.3	
	FT-IR	< LoD	13	
2009.05.15	Off-line DNPH	5.63	13.19	20.87
	PTR-TOF-MS m/z 31.018	3.5	27.1	22.5
	FT-IR	< LoD	14	12

[b] PTR-TOF-MS: LoD: <0.1 ppbV, error limits: +5/-50 % (calibrated; gas standard).
[c] FT-IR: LoD = 3 ppbV, error limits = max(3 ppbV; 5 %).

Acetaldehyde, **CH₃CHO (/ppbV)**

Date	Method	Sample 1	Sample 2	Sample 3
2009.05.10	Off-line DNPH	0.16	7.25	6.88
	PTR-TOF-MS[a] m/z 45.034	0.7	7.0	8.4
2009.05.11	Off-line DNPH	0.31	3.06	5.10
	PTR-TOF-MS m/z 45.034	0.5	3.1	4.8
2009.05.14	Off-line DNPH	0.41	16.70	
	PTR-TOF-MS m/z 45.034	2.7	17.9	
2009.05.15	Off-line DNPH	0.56	6.75	9.93
	PTR-TOF-MS m/z 45.034	3.1	5.1	7.4

[a]PTR-TOF-MS: LoD: <0.1 ppbV, data accuracy ± 10% (calibrated; gas standard).

Glycol aldehyde, **CH₂OHCHO (/ppbV)**

Date	Method	Sample 1	Sample 2	Sample 3
2009.05.10	Off-line DNPH	<0.1	1.73	2.02
	PTR-TOF-MS m/z 61.028	0.6	6.2	7.9
2009.05.11	Off-line DNPH	0.18	1.11	1.89
	PTR-TOF-MS m/z 61.028	0.4	2.3	3.5
2009.05.14	Off-line DNPH	0.58	6.40	
	PTR-TOF-MS m/z 61.028	0.5	10.4	
2009.05.15	Off-line DNPH	0.86	6.52	9.00
	PTR-TOF-MS m/z 61.028	0.9	5.9	9.0

[a]PTR-TOF-MS: LoD: <0.1 ppbV, data accuracy ± 25 % (estimated; ion-molecule reaction kinetics).

Formamide, **CHONH$_2$ (/ppbV)**

Date	Method	Sample 1	Sample 2	Sample 3
2009.05.10	Off-line Tenax TA			
	PTR-TOF-MS[b] m/z 46.029	0.8	17.6	16.6
2009.05.11	Off-line Tenax TA			
	PTR-TOF-MS m/z 46.029	0.8	6.0	7.5
2009.05.14	Off-line Tenax TA	<LoD	28.38	
	PTR-TOF-MS m/z 46.029	1.6	54.0	
2009.05.15	Off-line Tenax TA	<LoD	15.31	31.05
	PTR-TOF-MS m/z 46.029	2.1	34.5	37.7

[a] PTR-TOF-MS: LoD: <0.1 ppbV, data accuracy: ± 25 % (estimated; ion-molecule reaction kinetics).

MEA, H$_2$NCH$_2$CH$_2$OH, **(/ppbV)**

Date	Method	Sample 1	Sample 2	Sample 3
2009.05.10	Off-line	390	300	160
	PTR-TOF-MS[a] m/z 62.060	128	32	7
	FT-IR[b]	125	30	<LoD
	PTR-TOF-MS m/z 62.060			
2009.05.11	Off-line	3010	2240	1000
	PTR-TOF-MS m/z 62.060	88	40	16
	FT-IR	90	45	35
2009.05.14	Off-line	2690	760	
	PTR-TOF-MS m/z 62.060	732	91	
	FT-IR	625	90	
2009.05.15	Off-line	3050	960	640
	PTR-TOF-MS m/z 62.060	697	223	57
	FT-IR	600	210	75

[a] PTR-TOF-MS: LoD: <0.1 ppbV, data accuracy: ± 25 % (estimated; ion-molecule reaction kinetics). [b] FT-IR: LoD = 20 ppbV, error limits = max(20 ppbV; 15 %)

64

NILU – Norwegian Institute for Air Research

P.O. Box 100, N-2027 Kjeller, Norway

Associated with CIENS and the Environmental Research Alliance of Norway

ISO certified according to NS-EN ISO 9001

TITLE Atmospheric Degradationof Amines (ADA) Summary Report: Gas phase photo-oxidation of 2-aminoethanol (MEA)	PROJECT LEADER Claus Jørgen Nielsen
	NILU PROJECT NO. O-109011

AUTHOR(S) Claus Jørgen Nielsen, Barbara D'Anna, Christian Dye, Christian George, Martin Graus, Armin Hansel, Matthias Karl, Stephanie King, Mihayo Musabila, Marcus Müller, Norbert Schmidbauer, Yngve Stenstrøm, Armin Wisthaler	CLASSIFICATION * A
	CONTRACT REF. CLIMIT project no. 193438

REPORT PREPARED FOR

CLIMIT
Gassnova SF,
Dokkvegen 10,
N-3920 Porsgrunn2700

ABSTRACT

The gas phase photo-oxidation of 2-aminoethanol (MEA, $NH_2CH_2CH_2OH$) has been studied in a series of experiments at the European Photochemical Reactor, EUPHORE, in Valencia (Spain). The results show that the branching in the OH initiated H-abstraction reaction with $NH_2CH_2CH_2OH$ is: <10 % from $-NH_2$, >80 % from $-CH_2-$, and <10 % from $-CH_2OH$. The major products in the photo-oxidation are formamide, NH_2CHO, and formaldehyde, CH_2O. Amino acetaldehyde, NH_2CH_2CHO, and/or 2-imino ethanol, $HN=CHCH_2OH$, and 2-oxo acetamide, $NH_2C(O)CHO$ are formed as minor products. 2-(Nitroamino) ethanol, $O_2NNHCH_2CH_2OH$, has been unambiguously identified as a minor product in the MEA photo-oxidation. It is estimated that less than 3 ‰ of MEA emitted to the atmosphere will end up as the possibly carcinogenic nitramine in rural regions.

NORWEGIAN TITLE

Gassfase fotooksidasjon av 2-aminoetanol (MEA).

KEYWORDS		
2-Aminoethanol	Atmospheric chemistry	Nitramine formation

ABSTRACT (in Norwegian)

Fotooksidasjonen av 2-aminetanol (MEA, NH2CH2CH2OH) i gassfase har blitt studert i en rekke eksperimenter utført ved "European Photochemical Reactor" (EUPHORE) i Valencia i Spania. Resultatene viser at reaksjonsforgreininga i den OH-initierte H-abstraksjonsreaksjonen med $NH_2CH_2CH_2OH$ er: <10 % fra $-NH_2$, >80 % fra $-CH_2-$ og <10 % fra $-CH_2OH$. Hovedproduktene i fotooksidasjonen er formamid (NH_2CHO) og formaldehyd (CH_2O). Aminacetaldehyd (NH_2CH_2CHO) og/eller 2-iminetanol ($HN=CHCH_2OH$) og 2-oksoacetamid ($NH_2C(O)CHO$) er produkt som ble dannet i mindre mengder. 2-(Nitroamin)-etanol ($O_2NNHCH_2CH_2OH$) har blitt entydig identifisert som et produkt som blir dannet i mindre mengder i fotooksidasjonen av MEA. I landlige områder er det estimert at mindre enn 3 ‰ av mengden av MEA som blir sluppet ut i atmosfæren, vil ende opp som det mulige karsinogene stoffet nitramin.

* Classification	A	*Unclassified (can be ordered from NILU)*
	B	*Restricted distribution*
	C	*Classified (not to be distributed)*

NILU is an independent, nonprofit institution established in 1969. Through its research NILU increases the understanding of climate change, of the composition of the atmosphere, of air quality and of hazardous substances. Based on its research, NILU markets integrated services and products within analyzing, monitoring and consulting. NILU is concerned with increasing public awareness about climate change and environmental pollution.